Atmospheric Chemistry of Propionaldehyde: Kinetics and Mechanisms of Reactions with OH Radicals and Cl Atoms, UV Spectrum, and Self-Reaction Kinetics of $CH_3CH_2C(O)O_2$ Radicals at 298 K

Jean-Paul Le Crâne and Eric Villenave*

Laboratoire de Physico-Chimie Moléculaire, CNRS UMR 5803, Université Bordeaux I, 33405 Talence, Cedex, France

Michael D. Hurley,* Timothy J. Wallington, and James C. Ball

Ford Research Laboratory, MD 3083/SRL, Ford Motor Company, Dearborn, Michigan 48121-2053

Received: April 17, 2005; In Final Form: July 24, 2005

The kinetics and mechanism of the reactions of Cl atoms and OH radicals with CH_3CH_2CHO were investigated at room temperature using two complementary techniques: flash photolysis/UV absorption and continuous photolysis/FTIR smog chamber. Reaction with Cl atoms proceeds predominantly by abstraction of the aldehydic hydrogen atom to form acyl radicals. FTIR measurements indicated that the acyl forming channel accounts for (88 ± 5)%, while UV measurements indicated that the acyl forming channel accounts for (88 ± 3)%. Relative rate methods were used to measure: $k(Cl + CH_3CH_2CHO) = (1.20 \pm 0.23) \times 10^{-10}$; $k(OH + CH_3CH_2CHO) = (1.82 \pm 0.23) \times 10^{-11}$; and $k(Cl + CH_3CH_2C(O)Cl) = (1.64 \pm 0.22) \times 10^{-12}$ cm^3 molecule^{-1} s^{-1}. The UV spectrum of $CH_3CH_2C(O)O_2$, rate constant for self-reaction, and rate constant for cross-reaction with $CH_3CH_2O_2$ were determined: $\sigma(207\ nm) = (6.71 \pm 0.19) \times 10^{-18}$ cm^2 molecule^{-1}, $k(CH_3CH_2C(O)O_2 + CH_3CH_2C(O)O_2) = (1.68 \pm 0.08) \times 10^{-11}$, and $k(CH_3CH_2C(O)O_2 + CH_3CH_2O_2) = (1.20 \pm 0.06) \times 10^{-11}$ cm^3 molecule^{-1} s^{-1}, where quoted uncertainties only represent 2σ statistical errors. The infrared spectrum of $C_2H_5C(O)O_2NO_2$ was recorded, and products of the Cl-initiated oxidation of CH_3CH_2CHO in the presence of O_2 with, and without, NO_x were identified. Results are discussed with respect to the atmospheric chemistry of propionaldehyde.

1. Introduction

Propionaldehyde (CH_3CH_2CHO) is an important aldehyde in the atmosphere with concentrations reaching $1-2 \times 10^{10}$ molecules cm^{-3}.[1,2] It has both natural and anthropogenic sources, with small primary sources associated with vehicle exhaust and industrial activity and large secondary sources associated with the oxidation of volatile organic compounds.[3,4] Abstraction of the aldehydic H-atom by OH radicals gives propionyl radicals, $CH_3CH_2C(O)$, which combine with O_2 to give propionylperoxy radicals, $CH_3CH_2C(O)O_2$. As for acetylperoxy radicals, propionylperoxy radicals may play several important roles in atmospheric chemistry. $CH_3CH_2C(O)O_2$ radicals react rapidly with NO to give NO_2 which is then photolyzed leading to ozone formation. $CH_3CH_2C(O)O_2$ radicals react with NO_2 to form a stable peroxyacylnitrate ($CH_3CH_2C(O)O_2NO_2$). Peroxyacylnitrates are severe irritant compounds in photochemical smog and efficient reservoirs of NO_x in the troposphere and transport NO_x far from its sources.[5] In air masses with low NO_x concentration, acylperoxy radicals undergo reactions with HO_2 and other peroxy radicals. Reactions of acylperoxy radicals with HO_2 radicals are important radical chain termination reactions and are a source of ozone and carboxylic acids in the atmosphere.

The kinetic database concerning atmospherically relevant reactions of acylperoxy radicals is limited. Acetaldehyde is often used as the model for the reactivity of aldehydes in chemical modeling of atmospheric chemistry. Prior to a study of the effect of substitution of hydrogen atoms in $CH_3C(O)O_2$ by methyl groups on the reactivity of acylperoxy radicals with HO_2, it is first necessary to characterize a suitable laboratory source of acylperoxy radicals. In laboratory studies, Cl atoms or OH radicals are often used to generate peroxy radicals. Traditional OH radical sources, such as H_2O_2 or HNO_3 photolysis ($\lambda <$ 300 nm), are problematic because photolysis of aldehydes at wavelengths < 300 nm[6] can complicate the kinetic analysis. Chlorine atoms are produced readily by photolysis of Cl_2 at 330−360 nm where aldehyde photolysis is not a significant problem. The kinetics of the reactions of Cl atoms with aldehydes have been the subject of numerous studies, and the overall reaction kinetics are now reasonably well established.[7] Unfortunately, with the exception of acetaldehyde, pivalaldehyde, and isobutyraldehyde, there is little mechanistic information concerning the reaction of Cl atom with aldehydes. For acetaldehyde it has been shown that reaction occurs predominantly (>95%) via abstraction of the aldehydic hydrogen.[8,9] For pivalaldehyde and isobutyraldehyde we have shown that the acyl forming channel accounts for approximately 85% of the reaction.[10]

The objective of the present work was to determine the kinetics and mechanisms of the reactions of Cl atoms with CH_3CH_2CHO and to evaluate its utility as a source of methyl-substituted acyl and hence acylperoxy radicals.

* Corresponding author phone: 33 5 40 00 63 50; fax: 33 5 40 00 66 45; e-mail: e.villenave@lpcm.u-bordeaux1.fr.

10.1021/jp0519868 CCC: $30.25
Published on Web 11/25/2005

$$Cl + CH_3CH_2CHO \rightarrow HCl + CH_3CH_2C(O) \quad (1a)$$

$$\rightarrow HCl + CH_3CHCHO \quad (1b)$$

$$\rightarrow HCl + CH_2CH_2CHO \quad (1c)$$

Branching ratios for reaction 1 were investigated at room temperature using two complementary techniques: flash photolysis/UV absorption in Bordeaux and continuous photolysis/FTIR smog chamber in Dearborn. The UV spectrum and reactivity of the propionylperoxy radical were investigated using Br atoms as a source of radicals; reaction of Br atoms with aldehydes give acyl radicals in essentially 100% yield:

$$Br + CH_3CH_2CHO \rightarrow HBr + CH_3CH_2C(O) \quad (2)$$

To assess the possible importance of secondary reactions in the present system, relative rate studies were performed to determine rate constants for the reactions of Cl atoms with $CH_3CH_2C(O)Cl$. The infrared spectrum of $CH_3CH_2C(O)O_2NO_2$ was recorded, and product studies resulting from the reactivity of $CH_3CH_2C(O)O_2$ radicals in the presence of O_2 with and without NO_x species were conducted. Finally, the rate constant for the reaction of OH radicals with CH_3CH_2CHO was also measured and compared with previous works from the literature.

2. Experimental

The experimental systems used are described in detail elsewhere[11,12] and are discussed briefly here.

2.1. Flash Photolysis Experiments. A conventional flash photolysis UV absorption spectrometer was used to monitor peroxy radical absorptions at room temperature and atmospheric pressure. The reaction cell consists of a 70-cm-long, 4-cm-diameter Pyrex cylinder. A continuous flow of reactant gas mixture was irradiated periodically by two argon flash lamps. The analyzing beam was obtained from a deuterium lamp, passed once through the cell, dispersed using a monochromator (Jobin-Yvon, 2-nm-resolution), detected by a photomultiplier (R955 Hamamatsu), and transferred to a personal computer for averaging and analysis. Scattered light from the flash prevented data from being recorded for approximately 50−100 μs after the flash. About 30−40 absorption time profiles were acquired to reach a satisfactory signal-to-noise ratio. The total gas flow was adjusted so that the cell was replenished completely between flashes, thereby avoiding photolysis of reaction products. Decay traces were simulated by numerical integration of a set of differential equations that were representative of an appropriate chemical mechanism, and selected parameters (rate constants, absorption cross sections, and initial radical concentrations) were adjusted to give the best nonlinear least-squares fit.

Radicals were generated by photolysis of Cl_2 (or Br_2) at wavelengths longer than the Pyrex cutoff, using Cl_2 (or Br_2)/$CH_3CH_2CHO/O_2/N_2$ mixtures:

$$Cl_2 + h\nu \rightarrow 2Cl \text{ (for } \lambda > 280 \text{ nm)} \quad (3)$$

$$Cl + CH_3CH_2CHO \rightarrow HCl + \text{radicals} \quad (1)$$

$$Br_2 + h\nu \rightarrow 2Br \text{ (for } \lambda > 280 \text{ nm)} \quad (4)$$

$$Br + CH_3CH_2CHO \rightarrow HBr + \text{radicals} \quad (2)$$

Cl_2 and Br_2 were monitored using their absorption at 330 nm ($\sigma = 2.55 \times 10^{-19}$ cm^2 molecule^{-1} [13]) and 415 nm ($\sigma = 6.26 \times 10^{-19}$ cm^2 molecule^{-1} [14]), respectively. CH_3CH_2CHO was introduced into the reaction cell by bubbling a fraction of the diluent flow through liquid CH_3CH_2CHO maintained at constant temperature (273 K).

Acyl- and carbonyl-substituted-alkyl-peroxy radicals (hereafter, these are noted as alkyl-peroxy radicals) were formed by adding an excess of oxygen to ensure rapid and stoichiometric conversion of radicals formed via reaction 1 into peroxy radicals:

$$CH_3CH_2C(O) + O_2 + M \rightarrow CH_3CH_2C(O)O_2 + M \quad (5)$$

$$CH_3CHCHO + O_2 + M \rightarrow CH_3CHO_2CHO + M \quad (6)$$

$$CH_2CH_2CHO + O_2 + M \rightarrow CH_2O_2CH_2CHO + M \quad (7)$$

In Br atom initiated oxidation of CH_3CH_2CHO only one peroxy radical is formed: $CH_3CH_2C(O)O_2$. In Cl atom initiated oxidation all three peroxy radicals are generated.

Typical concentration ranges used were as follows: $[Cl_2] = (3-4) \times 10^{16}$ molecules cm^{-3} (Messer, 5% in N_2, purity > 99.9%), $[Br_2] = (1-3) \times 10^{15}$ molecules cm^{-3} (Acrôs Organics, 99.8%), $[CH_3CH_2CHO] = (0.55-2.22) \times 10^{16}$ molecules cm^{-3} (Aldrich, 99.5%), $[O_2] = 2.3 \times 10^{19}$ molecules cm^{-3} (Messer, 99.995%), $[N_2] = 1 \times 10^{18}$ molecules cm^{-3} (Messer, 99.999%). No UV absorbing products were generated when gas mixtures that contained all reactants except Cl_2 (or Br_2) were irradiated, which suggests that the present work is free from complications that are associated with the formation of absorbing radical species from the photolysis of the aldehydes.

2.2. Fourier Transform Infrared Smog Chamber System. Experiments were performed at room temperature (295 ± 1 K) in a 140-L Pyrex reactor interfaced to a Mattson Sirus 100 FTIR spectrometer.[12] The reactor was surrounded by 22 fluorescent blacklamps (GE F15T8-BL) which were used to photochemically initiate the experiments. Chlorine atoms were produced by photolysis of molecular chlorine.

$$Cl_2 + h\nu \rightarrow 2Cl \quad (3)$$

OH radicals were produced by the photolysis of CH_3ONO in air:

$$CH_3ONO + h\nu \rightarrow CH_3O + NO \quad (8)$$

$$CH_3O + O_2 \rightarrow HO_2 + HCHO \quad (9)$$

$$HO_2 + NO \rightarrow OH + NO_2 \quad (10)$$

Relative rate techniques were used to measure the rate constants of interest relative to a reference reaction whose rate constant has been established previously. Chlorine atom kinetics were studied using Cl_2/reactant/reference mixtures in air, or N_2, diluent. The relevant reactions in the system were 3, 11, and 12:

$$Cl + \text{reactant} \rightarrow \text{products} \quad (11)$$

$$Cl + \text{reference} \rightarrow \text{products} \quad (12)$$

Losses of reactant and reference are given by

$$\text{Ln}\left(\frac{[\text{reactant}]_{t_0}}{[\text{reactant}]_t}\right) = \frac{k_{11}}{k_{12}}\text{Ln}\left(\frac{[\text{reference}]_{t_0}}{[\text{reference}]_t}\right) \quad (\text{I})$$

where $[\text{reactant}]_{t_0}$, $[\text{reactant}]_t$, $[\text{reference}]_{t_0}$, and $[\text{reference}]_t$ are the concentrations of reactant and reference at times "t_o" and "t", and k_{11} and k_{12} are the rate constants for reactions 11 and

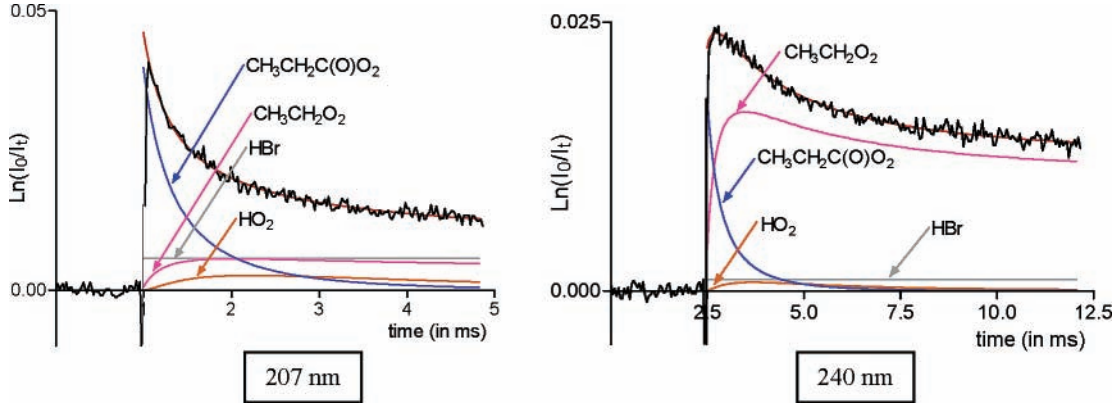

Figure 1. Decay traces at 207 and 240 nm following irradiation of $Br_2/CH_3CH_2CHO/O_2/N_2$ mixtures. Solid lines are results of simulations using the chemical mechanism detailed in Table 2.

12. Plots of $Ln([reactant]_{t_0}/[reactant]_t)$ versus $Ln([reference]_{t_0}/[reference]_t)$ should be linear, pass through the origin, and have a slope of k_{11}/k_{12}. Losses of reactant and the reference compounds were monitored by FTIR spectroscopy using an analyzing path length of 27 m and a resolution of 0.25 cm^{-1}. Infrared spectra were derived from 32 coadded interferograms. Gaseous reactants were introduced into the chamber via calibrated volumes. Liquid reactants were introduced into the chamber by transferring the vapor above the liquid into calibrated volumes. The contents of the calibrated volumes were swept into the chamber with the diluent gas (either air or nitrogen). All experiments were performed at 296 K. Reagents were obtained from commercial sources and were subjected to repeated freeze−pump−thaw cycling before use. In smog chamber experiments, it is important to check for an unwanted loss of reactants and products via photolysis, dark chemistry, and heterogeneous reactions. Control experiments were performed in which mixtures of reactants (except Cl_2 or CH_3ONO) in N_2 were subjected to UV irradiation for 15−30 min, and product mixtures obtained after the UV irradiation of reactant mixtures were allowed to stand in darkness in the chamber for 15 min. There was no observable loss of reactants or reference compounds, suggesting that photolysis, dark chemistry, and heterogeneous reactions are not a significant complication in the present work.

Propionic peracid, $CH_3CH_2C(O)OOH$, was prepared by reacting propionic anhydride with concentrated H_2O_2. Concentrated hydrogen peroxide was prepared from 50% commercial grade hydrogen peroxide by removing water-enriched-vapor under vacuum. A stoichiometric amount of propionic anhydride was added to the concentrated hydrogen peroxide (assumed to be 90%) assuming a molar ratio of 1:1 for the reaction of hydrogen peroxide and the propionic anhydride. We caution against using an excess of propionic anhydride due to the possible formation of potentially explosive peroxypropionic anhydride.[15]

3. Results

The results of studies of the (i) UV absorption spectrum of $CH_3CH_2C(O)O_2$, (ii) self-reaction kinetics of the $CH_3CH_2C(O)O_2$ radical, (iii) kinetics of the cross-reaction of $CH_3CH_2C(O)O_2$ with $CH_3CH_2O_2$, (iv) kinetics of reactions of Cl atoms with $CH_3CH_2C(O)Cl$ and CH_3CH_2CHO, (v) kinetics of the reaction of OH radicals with CH_3CH_2CHO, (vi) infrared spectrum of $CH_3CH_2C(O)O_2NO_2$, and (vii) products of the Cl atom initiated oxidation of CH_3CH_2CHO with, and without, NO_x species, are reported below.

TABLE 1: UV Absorption Cross Sections of the Propionylperoxy Radical/10^{-18} cm^2 $molecule^{-1}$

wavelength (in nm)	$CH_3CH_2C(O)O_2$
200	6.05 ± 0.30
205	6.53 ± 0.50
207	6.71 ± 0.19
210	6.40 ± 0.30
215	5.46 ± 0.09
220	4.32 ± 0.20
225	3.65 ± 0.31
230	3.22 ± 0.30
235	3.37 ± 0.18
240	3.30 ± 0.25
245	3.23 ± 0.12
250	2.81 ± 0.27
255	2.69 ± 0.31
260	2.11 ± 0.32
265	1.91 ± 0.24
270	1.39 ± 0.15
275	1.12 ± 0.25
280	0.78 ± 0.41

3.1. $CH_3CH_2C(O)O_2$: UV Absorption Spectrum, Self-Reaction Kinetics, and Kinetics of the Cross-Reaction with $CH_3CH_2O_2$. *3.1.1. UV Absorption Spectrum of the $CH_3CH_2C(O)O_2$ Radical.* To determine the branching ratio α_1 ($\alpha_1 = k_{1a}/k_1$) and develop a mechanism for the Cl-initiated oxidation of propionaldehyde, it was first necessary to determine the UV absorption of the $CH_3CH_2C(O)O_2$ radical and the kinetics of its self-reaction and cross-reaction with $CH_3CH_2O_2$. Bromine atoms were used as a clean source of propionylperoxy radicals. Abstraction of the aldehydic hydrogen is expected to occur from the reaction of Br atoms with CH_3CH_2CHO:

$$CH_3CH_2CHO + Br \rightarrow CH_3CH_2C(O) + HBr \quad (2)$$

$$CH_3CH_2C(O) + O_2 + M \rightarrow CH_3CH_2C(O)O_2 + M \quad (5)$$

In the presence of 710 Torr of O_2 at room temperature, addition of O_2 occurs rapidly (>99% complete within 0.1 μs).[16,17] Conversion of Br atoms into $CH_3CH_2C(O)O_2$ radicals is complete on a time scale that is essentially instantaneous when compared to that of the observations (see Figure 1). UV absorption cross sections of the $CH_3CH_2C(O)O_2$ radical were calibrated against those of the acetylperoxy radical[18] by replacing CH_3CH_2CHO by acetaldehyde under the same experimental conditions. As in the case of isobutyraldehyde $(CH_3)_2CHCHO$,[10] it was assumed that no decomposition of $CH_3CH_2C(O)$ occurs at 298 K with 710 Torr of O_2[16,17] and that all $CH_3CH_2C(O)$ radicals react with O_2 to form $CH_3CH_2C(O)O_2$ radicals. The

TABLE 2: Mechanism Used To Simulate the Flash Photolysis of $Br_2/CH_3CH_2CHO/N_2/O_2$ Mixtures at 298 K

no.	reactions	rate constants (in cm^3 $molecule^{-1}$ s^{-1})	ref
13	$2CH_3CH_2C(O)O_2 \rightarrow 2CH_3CH_2C(O)O + O_2$	$k_{13} = 1.68 \times 10^{-11}$	this work
14	$CH_3CH_2C(O)O + M \rightarrow CH_3CH_2 + CO_2 + M$	fast thermal decomposition	35
15	$CH_3CH_2 + O_2 + M \rightarrow CH_3CH_2O_2 + M$	$k_{15} = 7.8 \times 10^{-12}$	24
48a	$2CH_3CH_2O_2 \rightarrow 2CH_3CH_2O + O_2$	$k_{48} = 6.4 \times 10^{-14}$	35
48b	$\rightarrow CH_3CH_2OH + CH_3CHO + O_2$	$k_{48a}/k_{48} = 0.66$	35
39	$CH_3CH_2O + O_2 \rightarrow CH_3CHO + HO_2$	$k_{39} = 9.6 \times 10^{-15}$	24
49	$HO_2 + HO_2 \rightarrow H_2O_2 + O_2$	$k_{49} = 3 \times 10^{-12}$	24
16a	$CH_3CH_2C(O)O_2 + CH_3CH_2O_2 \rightarrow CH_3CH_2C(O)O + CH_3CH_2O + O_2$	$k_{16} = 1.2 \times 10^{-11}$	this work
16b	$\rightarrow CH_3CH_2C(O)OH + CH_3CHO + O_2$	$k_{16a}/k_{16} = 0.82$	this work
40a	$CH_3CH_2C(O)O_2 + HO_2 \rightarrow CH_3CH_2C(O)OOH + O_2$	$k_{40} = (1.4-2.5) \times 10^{-11}$	see discussion
40b	$\rightarrow CH_3CH_2C(O)OH + O_3$	$k_{40b}/k_{40} = 0.2^a$	53
41	$CH_3CH_2O_2 + HO_2 \rightarrow CH_3CH_2OOH + O_2$	$k_{41} = 7.6 \times 10^{-12}$	24

[a] Assumed the same as in the corresponding acetyl-peroxy radical reactions.

initial propionylperoxy radical concentration was assumed equal to the initial Br atom concentration.

The absorption cross sections of the $CH_3CH_2C(O)O_2$ radical have been measured in the range 200−280 nm. They are presented in Table 1 and were determined taking into account the initial absorption signal by extrapolating experimental curves to time zero integrating the chemical mechanism detailed in Table 2. The shape of the UV absorption spectrum of $CH_3CH_2C(O)O_2$, presented in Figure 2, is similar to that of the UV absorption spectra of the acetylperoxy,[18] isobutyrylperoxy,[16] and pivaloylperoxy[16] radicals: bimodal with a strong absorption band at 207 nm ($\sigma_{207} = 6.71 \times 10^{-18}$ cm^2 $molecule^{-1}$) and a weaker band around 240 nm ($\sigma_{240} = 3.30 \times 10^{-18}$ cm^2 $molecule^{-1}$). This absorption spectrum can be well-fitted using a double Gaussian function.

3.1.2. Kinetics of the Self-Reaction of the $CH_3CH_2C(O)O_2$ Radical and of Its Cross-Reaction with $CH_3CH_2O_2$. The $CH_3CH_2C(O)O_2$ self-reaction initiates a complex series of reactions which are detailed in Table 2.

$$CH_3CH_2C(O)O_2 + CH_3CH_2C(O)O_2 \rightarrow 2CH_3CH_2C(O)O + O_2 \quad (13)$$

$$CH_3CH_2C(O)O + M \rightarrow CH_3CH_2 + CO_2 + M \quad (14)$$

$$CH_3CH_2 + O_2 + M \rightarrow CH_3CH_2O_2 + M \quad (15)$$

$$CH_3CH_2C(O)O_2 + CH_3CH_2O_2 \rightarrow CH_3CH_2C(O)O + CH_3CH_2O + O_2 \quad (16a)$$

$$\rightarrow CH_3CH_2C(O)OH + CH_3CHO + O_2 \quad (16b)$$

Decay traces were recorded at two wavelengths, 207 and 240 nm, corresponding to absorption maxima of $CH_3CH_2C(O)O_2$ and $CH_3CH_2O_2$[18] radicals, respectively. The $CH_3CH_2C(O)O_2$ self-reaction rate constant was determined by monitoring at 207 nm where absorption by $CH_3CH_2C(O)O_2$ dominates. The rate constant for reaction 16 and its branching ratio ($\alpha_{16} = k_{16a}/k_{16}$) were determined by monitoring at 240 nm where both $CH_3CH_2C(O)O_2$ and $CH_3CH_2O_2$[18] absorb strongly.

Decay traces were simulated by taking the complete chemical mechanism into account (see Table 2). The rate constants of the $CH_3CH_2C(O)O_2$ self-reaction and of the ($CH_3CH_2C(O)O_2 + CH_3CH_2O_2$) cross-reaction, and its branching ratio α_{16}, were adjusted to fit the decay traces. They are presented in Table 3. Eleven determinations of k_{13}, k_{16}, and α_{16} were performed, resulting in the following rate constants at room temperature:

$$k_{13} = (1.68 \pm 0.08) \times 10^{-11} \text{ cm}^3 \text{ molecule}^{-1} \text{ s}^{-1}$$

and

$$k_{16} = (1.20 \pm 0.06) \times 10^{-11} \text{ cm}^3 \text{ molecule}^{-1} \text{ s}^{-1} \text{ with } \alpha_{16} = (0.82 \pm 0.04)$$

where quoted uncertainties only represent 2σ statistical errors. The global uncertainties on the rate constant values are discussed in the section 4.1.

The measured value of α_{16} is very close to the arithmetic average of the α values (where α is the ratio of the rate constant for the alkoxy channel to the total self-reaction rate constant) for the corresponding self-reactions.

3.2. Relative Rate Study of the Reaction of Cl Atoms with $CH_3CH_2C(O)Cl$. Prior to the study of propionaldehyde, the relative rate technique was used to measure the reactivity of Cl atoms with propionyl chloride, $CH_3CH_2C(O)Cl$. The kinetics of reaction 17 was measured relative to reactions 18 and 19.

$$Cl + CH_3CH_2C(O)Cl \rightarrow \text{products} \quad (17)$$

$$Cl + CH_3CH_2Cl \rightarrow \text{products} \quad (18)$$

$$Cl + CH_3OCHO \rightarrow \text{products} \quad (19)$$

Reaction mixtures consisted of 14−22 mTorr of $CH_3CH_2C(O)Cl$, 99−203 Torr of Cl_2, and 22−31 mTorr of ethyl chloride CH_3CH_2Cl or 4−9 mTorr of methyl formate CH_3OCHO in 700 Torr of N_2. Figure 3a shows the loss of $CH_3CH_2C(O)Cl$ versus the loss of the reference compounds in the presence of Cl atoms. Linear least-squares analysis of the data in Figure 3a gives $k_{17}/k_{18} = 0.20 \pm 0.01$ and $k_{17}/k_{19} = 1.20 \pm 0.06$. Quoted uncertainties are two standard deviations from the linear regressions. Potential uncertainties in the reference rate constant add an additional 10% uncertainty to k_{17}. Using $k_{18} = 8.0 \times 10^{-12}$ cm^3 $molecule^{-1}$ s^{-1} [19] and $k_{19} = 1.4 \times 10^{-12}$ cm^3 $molecule^{-1}$ s^{-1} [20] and combining uncertainties associated with the rate constant ratios and reference rate constants, we derive $k_{17} = (1.60 \pm 0.18) \times 10^{-12}$ cm^3 $molecule^{-1}$ s^{-1} and $(1.67 \pm 0.19) \times 10^{-12}$ cm^3 $molecule^{-1}$ s^{-1}. Results obtained using two different reference compounds were, within the experimental uncertainties, indistinguishable, suggesting the absence of significant systematic errors in the present work. We choose to cite a final value for k_{17} which is the average of the two determinations with error limits which include the extremes of the individual determinations, $k_{17} = (1.64 \pm 0.22) \times 10^{-12}$ cm^3 $molecule^{-1}$ s^{-1}.

3.3. Relative Rate Study of the Reaction of CH_3CH_2CHO with Cl Atoms and OH Radicals. *3.3.1. Reaction of CH_3CH_2CHO with Cl Atoms.* The kinetics of reaction 1 was

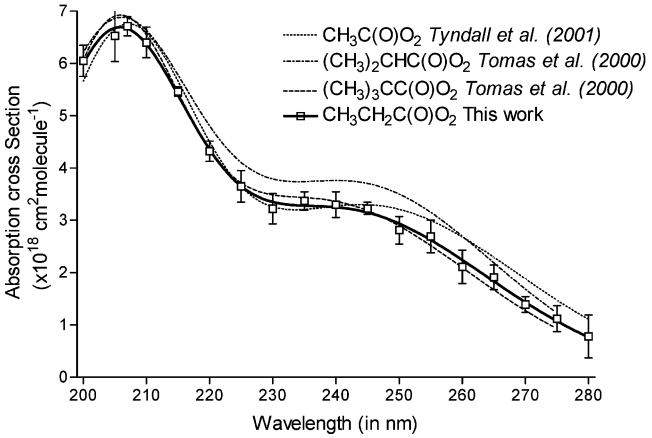

Figure 2. UV spectrum of the $CH_3CH_2C(O)O_2$ radical between 200 and 280 nm. Solid line represents the fit of experimental data using the following double Gaussian expression: $\sigma(CH_3CH_2C(O)O_2) = 5.6 \times \exp\{-0.5 \times [(\lambda - 204.3)/11.2]^2\} + 3.22 \times \exp\{-0.5 \times [(\lambda - 239.9)/23.7]^2\}$ with σ expressed in 10^{-18} cm^2 $molecule^{-1}$ and λ in nm. UV absorption spectra of $CH_3C(O)O_2$, $(CH_3)_2CHC(O)O_2$, and $(CH_3)_3CC(O)O_2$ radicals are shown for comparison.

TABLE 3: Rate Constants ($/10^{-11}$ cm^3 $molecule^{-1}$ s^{-1}) for the $CH_3CH_2C(O)O_2$ Radical Self-Reaction (k_{13}), Cross-Reaction with $CH_3CH_2O_2$ (k_{16}), and the Branching Ratio (α_{16})

expt no.	k_{13}	k_{16}	α_{16}
1	1.61	1.16	0.744
2	1.82	1.24	0.812
3	1.71	1.23	0.864
4	1.72	1.19	0.824
5	1.52	1.27	0.937
6	1.81	1.27	0.848
7	1.62	1.16	0.748
8	1.85	1.24	0.769
9	1.62	1.14	0.807
10	1.64	1.27	0.765
11	1.54	0.99	0.848
mean	1.68 ± 0.08	1.20 ± 0.06	0.82 ± 0.04

measured relative to reactions 20−22.

$$Cl + CH_3CH_2CHO \rightarrow \text{products} \quad (1)$$

$$Cl + C_2H_6 \rightarrow \text{products} \quad (20)$$

$$Cl + C_2H_4 \rightarrow \text{products} \quad (21)$$

$$Cl + C_3H_8 \rightarrow \text{products} \quad (22)$$

Reaction mixtures consisted of 73−76 mTorr of CH_3CH_2CHO, 103−148 mTorr of Cl_2, and either 148, 13.1, or 100 mTorr of ethane, ethene, or propane, respectively, in 700 Torr of N_2. Figure 3b shows the loss of CH_3CH_2CHO versus the reference compounds in the presence of Cl atoms. Linear least-squares analysis of the data in Figure 3b gives $k_1/k_{20} = 2.14 \pm 0.07$, $k_1/k_{21} = 1.38 \pm 0.06$, and $k_1/k_{22} = 0.795 \pm 0.055$. Quoted uncertainties are two standard deviations from the linear regressions. Potential uncertainties in the reference rate constant add an additional 10% uncertainty to k_1. Using $k_{20} = 5.7 \times 10^{-11}$ cm^3 $molecule^{-1}$ s^{-1},[21] $k_{21} = 9.3 \times 10^{-11}$ cm^3 $molecule^{-1}$ s^{-1},[22] and $k_{22} = 1.4 \times 10^{-10}$ cm^3 $molecule^{-1}$ s^{-1} [21] and combining uncertainties associated with the measured rate constant ratios and the reference rate constants, we derive $k_1 = (1.22 \pm 0.13) \times 10^{-10}$, $(1.28 \pm 0.14) \times 10^{-10}$, and $(1.11 \pm 0.14) \times 10^{-10}$ cm^3 $molecule^{-1}$ s^{-1}. Results obtained using three different reference compounds were, within the experimental uncertainties, indistinguishable, suggesting the absence of significant systematic errors in the present work. We choose to cite a final value for k_1 which is the average of the three determinations with error limits which include the extremes of the individual determinations, $k_1 = (1.20 \pm 0.23) \times 10^{-10}$ cm^3 $molecule^{-1}$ s^{-1}.

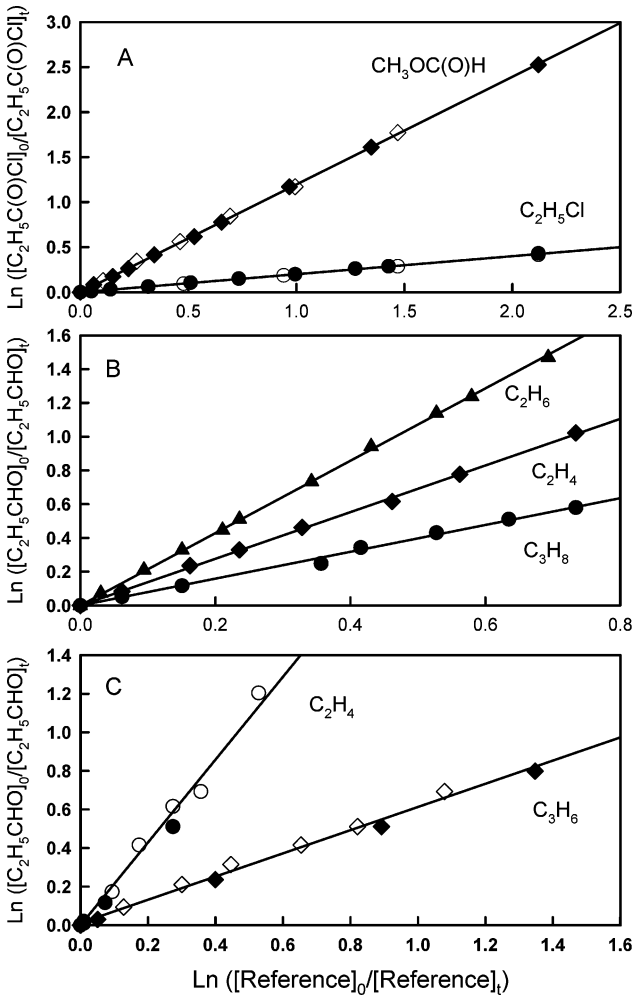

Figure 3. Panel A: loss of $CH_3CH_2C(O)Cl$ versus CH_3OCHO (diamonds) and CH_3CH_2Cl (circles) following UV irradiation of $CH_3CH_2C(O)Cl$/reference/Cl_2 mixtures in N_2. Panel B: loss of CH_3CH_2CHO versus C_2H_6 (triangles), C_2H_4 (diamonds), and C_3H_8 (circles) following UV irradiation of CH_3CH_2CHO/reference/Cl_2 mixtures in N_2. Panel C: loss of CH_3CH_2CHO versus C_2H_4 (circles) and C_3H_6 (diamonds) following UV irradiation of CH_3CH_2CHO/reference/CH_3ONO/NO mixtures in air. All experiments were performed in 700 Torr total pressure and 296 K.

3.3.2. Reaction of CH_3CH_2CHO with OH Radicals. The kinetics of reaction 23 was measured relative to reactions 24 and 25.

$$OH + CH_3CH_2CHO \rightarrow \text{products} \quad (23)$$

$$OH + C_2H_4 \rightarrow \text{products} \quad (24)$$

$$OH + C_3H_6 \rightarrow \text{products} \quad (25)$$

Reaction mixtures consisted of 35−102 mTorr of CH_3CH_2CHO, 93−206 mTorr of CH_3ONO, 27−56 mTorr of NO, and 5−15 mTorr of ethene or 15−17 mTorr of propene in 700 Torr of air. Figure 3c shows the loss of CH_3CH_2CHO versus the loss of the reference compounds in the presence of OH radicals. Linear least-squares analysis of the data in Figure 3c gives k_{23}/

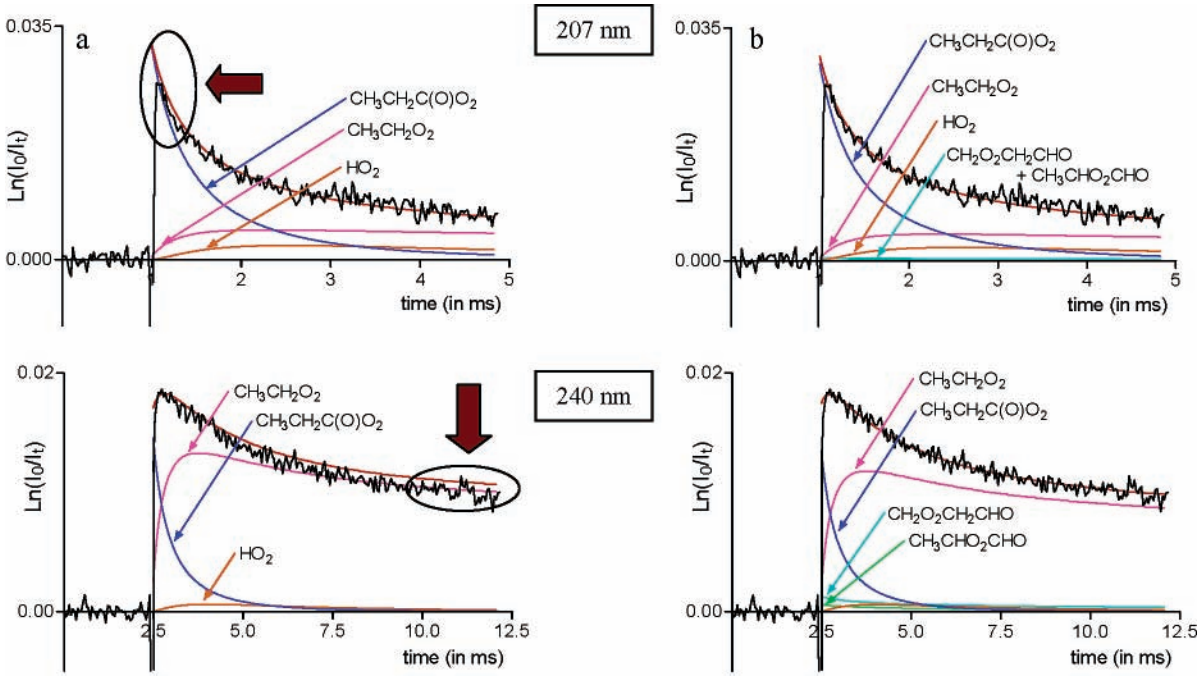

Figure 4. Decay traces at 207 and 240 nm following UV irradiation of $Cl_2/CH_3CH_2CHO/O_2/N_2$ mixtures. Solid lines are results of simulations assuming either 100% conversion of Cl atoms into $CH_3CH_2C(O)O_2$ radicals (a) or 88% conversion into $CH_3CH_2C(O)O_2$, 6% into $CH_2O_2CH_2CHO$, and 6% into CH_3CHO_2CHO radicals (b).

$k_{24} = 2.14 \pm 0.17$ and $k_{23}/k_{25} = 0.614 \pm 0.037$. Quoted uncertainties are two standard deviations from the linear regressions. Potential uncertainties in the reference rate constant add an additional 10% uncertainty to k_{23}. Using $k_{24} = 8.7 \times 10^{-12}$ cm^3 molecule^{-1} s^{-1} [23] and $k_{25} = 2.9 \times 10^{-11}$ cm^3 molecule^{-1} s^{-1} [24] and combining uncertainties, we derive $k_{23} = (1.86 \pm 0.21) \times 10^{-11}$ cm^3 molecule^{-1} s^{-1} and $(1.78 \pm 0.19) \times 10^{-11}$ cm^3 molecule^{-1} s^{-1}. Results obtained using two different reference compounds were, within the experimental uncertainties, indistinguishable, suggesting the absence of significant systematic errors in the present work. We choose to cite a final value for k_{23} which is the average of the two determinations with error limits which include the extremes of the individual determinations, $k_{23} = (1.82 \pm 0.23) \times 10^{-11}$ cm^3 molecule^{-1} s^{-1}.

3.4. Mechanism of the Reaction of Cl Atoms with CH_3CH_2CHO. *3.4.1. Flash Photolysis Experiments.* As for isobutyraldehyde,[10] the reaction of chlorine atoms with CH_3CH_2CHO leads to the formation of both acyl and alkyl radicals which, in the presence of O_2, leads to the formation of three different peroxy radicals ($CH_3CH_2C(O)O_2$, CH_3CHO_2CHO, and $CH_2O_2CH_2CHO$). In the presence of 710 Torr of O_2 at room temperature, addition of O_2 occurs rapidly (>99% complete within 0.1 μs) and is essentially the sole fate of the acyl and alkyl radicals formed in reaction 1.[16,17] Hence, conversion of Cl atoms into peroxy radicals is complete on a time scale that is much shorter than the observations (see Figure 4). The method used to determine the branching ratio $\alpha_1 = k_{1a}/k_1$ (corresponding to the channel forming acyl radicals) was based on the difference in acyl- and alkylperoxy radical absorptions in the 200−300 nm wavelength range, as already described in a previous work.[10] Acylperoxy radicals, such as $CH_3CH_2C(O)O_2$, have bimodal spectra (see Figure 2) with maxima near 207 and 240 nm, whereas alkylperoxy radicals, such as $CH_2O_2CH_2CHO$, have monomodal spectra with a maximum near 240 nm. Decay traces were recorded at 207 and 240 nm. In a first approach, only the initial formation of $CH_3CH_2C(O)O_2$ radical was considered (as with Br-initiated oxidation of propionaldehyde) but decay traces could not be simulated adequately with the chemical model presented in Table 2 (see Figure 4a). Consequently, formations of the CH_3CHO_2CHO and $CH_2O_2CH_2CHO$ radicals were also considered. The sensitivity of the results to the CH_3CHO_2CHO and $CH_2O_2CH_2CHO$ radical reactions used in the chemical model (see Tables 2 and 4) is discussed in section 4.1. The total initial radical concentration was fixed, and the proportion of $CH_3CH_2C(O)O_2$, CH_3CHO_2CHO, and $CH_2O_2CH_2CHO$ radicals was varied to achieve the best fit to the experimental data at both 207 and 240 nm (see Figure 4b). The branching ratio between CH_2CH_2CHO and CH_3CHCHO formation was based upon data for the Cl + $CH_3CH_2C(O)CH_2CH_3$ reaction.[10]

The best fit was achieved with 88% initial formation of the $CH_3CH_2C(O)O_2$ radical, yielding $\alpha_1 = k_{1a}/k_1 = (0.88 \pm 0.03)$. It is possible that $CH_3CH_2C(O)$ radicals formed in reaction 1a possess sufficient chemical activation to undergo prompt decomposition. Such prompt decomposition would lead to the formation of $CH_3CH_2O_2$ radicals in the system. To investigate this possibility, simulations were performed in which $CH_3CH_2C(O)O_2$ were replaced with $CH_3CH_2O_2$ radicals. Experimental decays could not be simulated satisfactorily using such a mechanism, and we estimate that <3% of $CH_3CH_2C(O)$ radicals undergo prompt decomposition.

In addition, the self-reaction rate constant of the $CH_3CH_2C(O)O_2$ radical was determined to compare its value with that measured above using Br atoms as initiator. Decay traces were simulated by taking the complete chemical mechanism into account (Tables 2 and 4). The rate constant of the $CH_3CH_2C(O)O_2$ radical self-reaction was adjusted to fit the decay traces. The unknown rate constants for the cross-reactions between all peroxy RO_2 and acylperoxy $RC(O)O_2$ radicals were estimated from previous SARs on peroxy radical cross-reactions.[25,26] Six determinations of k_{13} were performed, resulting in the following rate constant at room temperature:

$$k_{13} = (1.67 \pm 0.08) \times 10^{-11}\ \text{cm}^3\,\text{molecule}^{-1}\,\text{s}^{-1}$$

TABLE 4: Reactions Added to Mechanism in Table 2 To Account for $CH_2O_2CH_2CHO$ and CH_3CHO_2CHO Radicals in Flash Photolysis Experiments Using $Cl_2/CH_3CH_2CHO/N_2/O_2$ Mixtures

no.	reactions		rate constants (in cm^3 $molecule^{-1}$ s^{-1})	ref
50a	$2CH_2O_2CH_2CHO$	$\rightarrow 2CH_2OCH_2CHO + O_2$	$k_{50} = 2 \times 10^{-12}$	see discussion
50b		$\rightarrow CH_2OHCH_2CHO + CHOCH_2CHO + O_2$	$k_{50a}/k_{50} = 0.66^b$	35
51	$CH_2OCH_2CHO + O_2$	$\rightarrow CHOCH_2CHO + HO_2$	$k_{51} = 9.7 \times 10^{-15b}$	26
52a	$CH_2O_2CH_2CHO + CH_3CH_2C(O)O_2$	$\rightarrow CH_2OCH_2CHO + (CH_3)_2CHC(O)O + O_2$	$k_{52} = 1.4 \times 10^{-11b}$	25
52b		$\rightarrow CHOCH_2CHO + CH_3CH_2C(O)OH$	$k_{52a}/k_{52} = 0.8^b$	25
53a	$CH_2O_2CH_2CHO + CH_3CH_2O_2$	$\rightarrow CH_2OCH_2CHO + CH_3CH_2O + O_2$	$k_{53} = 1.1 \times 10^{-12a}$	25
		$\rightarrow$ molecular products	$k_{53a}/k_{53} = 0.66^a$	25
54	$CH_2O_2CH_2CHO + HO_2$	$\rightarrow CH_2OOHCH_2CHO + O_2$	$k_{54} = 1.0 \times 10^{-11b}$	25
55a	$CH_2O_2CH_2CHO + CH_3CHO_2CHO$	$\rightarrow CH_2OCH_2CHO + CH_3CHOCHO + O_2$	$k_{55} = 1.0 \times 10^{-12b}$	25
		$\rightarrow$ molecular products	$k_{55a}/k_{55} = 0.56^b$	25
56a	$2CH_3CHO_2CHO$	$\rightarrow 2CH_3CHOCHO + O_2$	$k_{56} = 2.0 \times 10^{-12}$	see discussion
56b		$\rightarrow CH_3C(O)CHO + CH_3C(OH)HCHO + O_2$	$k_{56a}/k_{56} = 0.56^b$	35
57	$CH_3CHOCHO + O_2$	$\rightarrow CH_3C(O)CHO + HO_2$	$k_{57} = 7.7 \times 10^{-15b}$	54
58a	$CH_3CHO_2CHO + CH_3CH_2C(O)O_2$	$\rightarrow CH_3CHOCHO + (CH_3)_2CHC(O)O + O_2$	$k_{58} = 1 \times 10^{-11b}$	35
58b		$\rightarrow CH_3C(O)CHO + (CH_3)_2CHC(O)OH + O_2$	$k_{58a}/k_{58} = 0.35^b$	35
59a	$CH_3CHO_2CHO + CH_3CH_2O_2$	$\rightarrow (CH_3)_2COCHO + (CH_3)_3CO + O_2$	$k_{59} = 8 \times 10^{-13b}$	25
59b		$\rightarrow$ molecular products	$k_{59a}/k_{59} = 0.60^b$	25
60	$CH_3CHO_2CHO + HO_2$	$\rightarrow CH_3C(OOH)HCHO + O_2$	$k_{60} = 5.2 \times 10^{-12a,\,b}$	35

[a] Assumed to be similar to the corresponding acetyl- or methyl-peroxy radical reactions. [b] Considered to be similar as that of the corresponding propyl-, isopropyl-peroxy radical reactions.

This value is in very good agreement with that determined in section 3.1, using Br atoms to generate $CH_3CH_2C(O)O_2$ radicals.

3.4.2. FTIR Experiments. Experiments to investigate the mechanism of reaction 1 were conducted using the UV irradiation of mixtures of CH_3CH_2CHO and Cl_2, in N_2 diluent. Initial concentrations were 26−37 mTorr of CH_3CH_2CHO and 100−400 mTorr of Cl_2, in 700 Torr of N_2. In such experiments, $CH_3CH_2C(O)Cl$, $CH_3CHClCHO$, and CH_2ClCH_2CHO are expected to be produced by the following sequence of reactions:

$$Cl + CH_3CH_2CHO \rightarrow CH_3CH_2C(O) + HCl \quad (1a)$$

$$Cl + CH_3CH_2CHO \rightarrow CH_3CHCHO + HCl \quad (1b)$$

$$Cl + CH_3CH_2CHO \rightarrow CH_2CH_2CHO + HCl \quad (1c)$$

$$Cl_2 + CH_3CH_2C(O) \rightarrow CH_3CH_2C(O)Cl + Cl \quad (26)$$

$$Cl_2 + CH_3CHCHO \rightarrow CH_3CHClCHO + Cl \quad (27)$$

$$Cl_2 + CH_2CH_2CHO \rightarrow CH_2ClCH_2CHO + Cl \quad (28)$$

The yields of $CH_3CH_2C(O)Cl$, $CH_3CHClCHO$, and CH_2ClCH_2CHO provide a measure of the importance of channels 1a−c. Of the three isomeric chlorides, only $CH_3CH_2C(O)Cl$ is commercially available. $CH_3CH_2C(O)Cl$ was observed as the major primary product formed from the reaction of CH_3CH_2CHO with Cl in N_2. $CH_3CH_2C(O)Cl$ also reacts with Cl via reaction 17. The concentration profile of a reactive primary product can be described[27] by the expression

$$\frac{[CH_3CH_2C(O)Cl]_t}{[CH_3CH_2CHO]_{t_0}} = \left\{\frac{\alpha_1}{(1-(k_{17}/k_1))}\right\}(1-x)\{(1-x)^{((k_{17}/k_1)-1)} - 1\} \quad \text{(II)}$$

where $x = 1 - ([CH_3CH_2CHO]_t/[CH_3CH_2CHO]_{t_0})$ (the fractional consumption of CH_3CH_2CHO at time t) and α_1 is the yield of $CH_3CH_2C(O)Cl$ from the reaction of Cl with CH_3CH_2CHO. Figure 5 shows a plot of $[CH_3CH_2C(O)Cl]_t/[CH_3CH_2CHO]_{t_0}$ versus $[CH_3CH_2CHO]_t/[CH_3CH_2CHO]_{t_0}$ in three different experiments. Using the values for k_{17} and k_1 determined in this study, $(k_{17}/k_1) = 0.0137$, and a fit of eq II to the data in Figure 5 gives $\alpha_1 = 0.88 \pm 0.05$. Abstraction of the aldehydic hydrogen, reaction 1a, accounts for 88% of the reaction of Cl atoms with propionaldehyde. The other abstraction channels, reactions 1b and 1c, are minor channels accounting for 12% of the total reaction 1.

3.5. Determination of the Gas-Phase Dimerization Constant for $CH_3CH_2C(O)OH$. Propionic acid, $CH_3CH_2C(O)OH$, is a possible product in the Cl initiated oxidation of CH_3CH_2CHO, and a calibrated reference spectrum was required for analysis. Carboxylic acids form cyclic dimers[28−30]

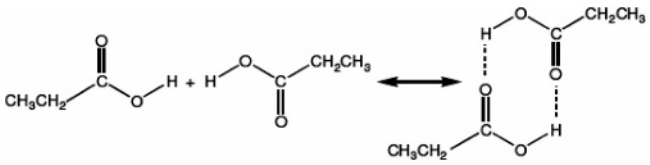

and the generation of a calibrated reference spectrum required knowledge of the dimerization constant. The observed pressure of $CH_3CH_2C(O)OH$ vapor is expressed as

$$P_{obs} = P_M + P_D = P_M + K_d P_M^2 \quad \text{(III)}$$

where P_M is the pressure of the monomer, P_D is the pressure of the dimer, and K_d is the dimerization constant. If dimerization occurs in the calibrated volume and the dimer dissociates upon expansion into the chamber, the acid concentration in the chamber will be higher than calculated assuming only the monomer in the calibrated volume. To correct for dimer formation in the calibrated volume, the dimerization constant was determined for propionic acid. For the dimerization constant measurements, propionic acid vapor was introduced into a small cell with a diameter of 4.5 cm and a length of 17.75 cm, filled to 700 Torr total pressure with nitrogen, and placed in the IR beam, and the FTIR spectrum was acquired. This procedure was repeated using different pressures of the acid vapor. As expected, the fraction of the acid present as the dimer increased as the concentration of acid was increased. Since the monomer and dimer are present in different relative amounts in spectra acquired using different concentrations of acid, the monomer

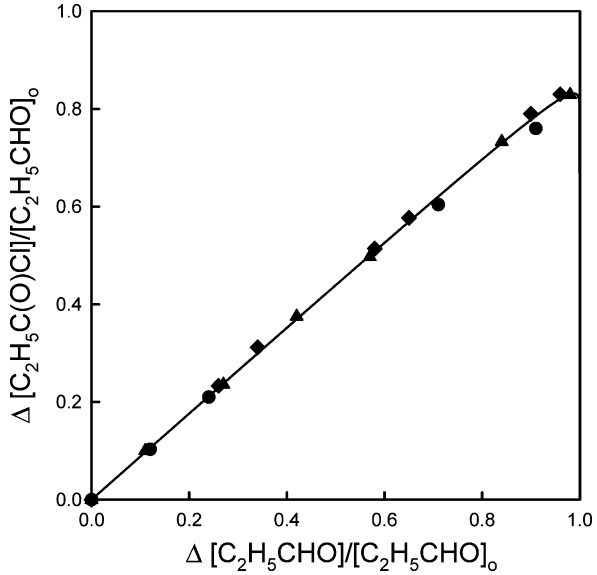

Figure 5. Formation of $CH_3CH_2C(O)Cl$ versus loss of CH_3CH_2CHO, normalized for the initial aldehyde concentration. Three experiments were performed in which mixtures of CH_3CH_2CHO and Cl_2 were irradiated in 700 Torr of N_2 diluent. The line through the data is a fit of eq II to the data. The rate constant ratio k_{17}/k_1 was fixed at 0.0137, and the fit of eq II to the data gives a chloride yield of (88 ± 5)%.

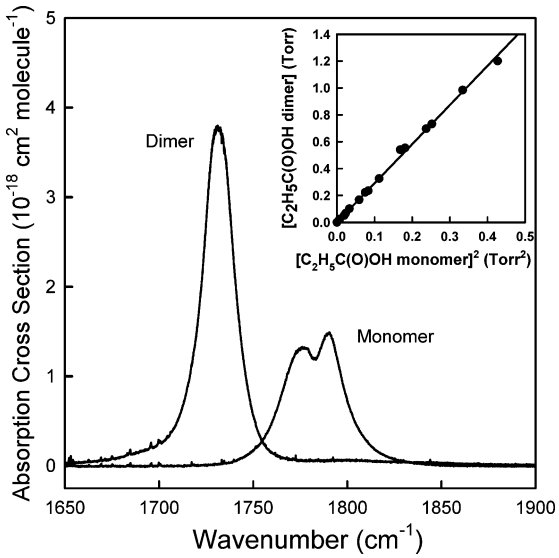

Figure 6. IR spectra for the carbonyl feature of the $CH_3CH_2C(O)OH$ monomer and dimer. The insert shows the dimer concentration versus the square of the monomer concentration. The slope is the dimerization constant, $K_d = 2.91 \pm 0.31$ Torr^{-1}.

and dimer spectra can be separated and quantified. Figure 6 shows the carbonyl region of the IR spectrum for the propionic acid monomer and dimer.

From eq III, a plot of P_D vs P_M^2 is expected to be linear, pass through the origin, and have a slope that is the dimerization constant, K_d. The insert in Figure 6 shows this plot for $CH_3CH_2C(O)OH$. The line through the data is a linear least-squares fit which gives $K_d = 2.91 \pm 0.31$ Torr^{-1}. This dimerization constant was used to account for the dimer formation in our calibrated volume during the introduction of propionic acid into the chamber.

It is of interest to note that our equilibrium constant is approximately a factor of 2.6 larger than that reported previously by Clague and Bernstein.[31] The origin of this discrepancy is unknown.

3.6. Product Study of the Cl-Initiated Oxidation of CH_3CH_2CHO. A product study of the Cl-initiated oxidation of CH_3CH_2CHO in the absence of NO_x was conducted to provide insight into the atmospheric oxidation of propionaldehyde. Two experiments were conducted using initial concentrations of either 37.8 mTorr of CH_3CH_2CHO and 100 mTorr of Cl_2 in 700 Torr of air or 100.3 mTorr of CH_3CH_2CHO and 216 mTorr of Cl_2 in 700 Torr of air. Figure 7 shows the products formed during the irradiation of 100.3 mTorr of CH_3CH_2CHO and 216 mTorr of Cl_2 in 700 Torr of air. There was no evidence for formation of CO as a primary product (<3% yield) confirming the assumption in section 3.4.1 that reaction with O_2 is the fate of $CH_3CH_2C(O)$ radicals. Figure 7a shows the primary products observed: CH_3CHO, CH_3CH_2OOH, $CH_3CH_2C(O)OH$, and $CH_3CH_2C(O)OOH$. Figure 7b shows the secondary (or possibly tertiary) products observed: HC(O)H, HC(O)OH, CH_3OOH, CH_3OH, $CH_3C(O)OH$, and $CH_3C(O)OOH$. The curved primary product profiles are characteristic of reactive products. Equation II can be fit to the data in Figure 7a, using the yields and rate constant ratios as fit parameters, for the following reactions:

$$CH_3CH_2CHO + Cl \rightarrow \alpha CH_3CHO + \text{products} \quad (29)$$

$$CH_3CHO + Cl \rightarrow \text{products} \quad (30)$$

$$CH_3CH_2CHO + Cl \rightarrow \beta CH_3CH_2OOH + \text{products} \quad (31)$$

$$CH_3CH_2OOH + Cl \rightarrow \text{products} \quad (32)$$

$$CH_3CH_2CHO + Cl \rightarrow \gamma CH_3CH_2C(O)OH + \text{products} \quad (33)$$

$$CH_3CH_2C(O)OH + Cl \rightarrow \text{products} \quad (34)$$

$$CH_3CH_2CHO + Cl \rightarrow \delta CH_3CH_2C(O)OOH + \text{products} \quad (35)$$

$$CH_3CH_2C(O)OOH + Cl \rightarrow \text{products} \quad (36)$$

In these reactions α, β, γ, and δ are the initial yields of CH_3CHO, CH_3CH_2OOH, $CH_3CH_2C(O)OH$, and $CH_3CH_2C(O)OOH$, respectively, following the Cl atom initiated oxidation of CH_3CH_2CHO. It should be noted that the processes indicated by reactions 29−36 are multiple reactions. Figure 8 shows a plot of $[\text{products}]_t/[CH_3CH_2CHO]_{t_0}$ versus $\Delta[CH_3CH_2CHO]_t/[CH_3CH_2CHO]_{t_0}$ for two experiments. The parameters in eq II that give the best fits are as follows: $\alpha = 0.51 \pm 0.01$ and $k_{30}/k_1 = 0.45 \pm 0.03$ for CH_3CHO, $\beta = 0.24 \pm 0.01$ and $k_{32}/k_1 = 0.58 \pm 0.06$ for CH_3CH_2OOH, $\gamma = 0.04 \pm 0.002$ and $k_{34}/k_1 = 0.008 \pm 0.028$ for $CH_3CH_2C(O)OH$, $\delta = 0.08 \pm 0.002$ and $k_{36}/k_1 = 0.058 \pm 0.02$ for $CH_3CH_2C(O)OOH$.

3.6.1. CH_3CHO as a Primary Product. The observation of CH_3CHO as a primary product of the Cl initiated oxidation of CH_3CH_2CHO is consistent with reaction 1a followed by reaction with oxygen to form the propionylperoxy radical, $CH_3CH_2C(O)O_2$

$$CH_3CH_2C(O) + O_2 + M \rightarrow CH_3CH_2C(O)O_2 + M \quad (5)$$

The propionylperoxy radical reacts with other peroxy radicals to give the alkoxy radical, $CH_3CH_2C(O)O$:

$$CH_3CH_2C(O)O_2 + RO_2 \rightarrow CH_3CH_2C(O)O + RO + O_2 \quad (37)$$

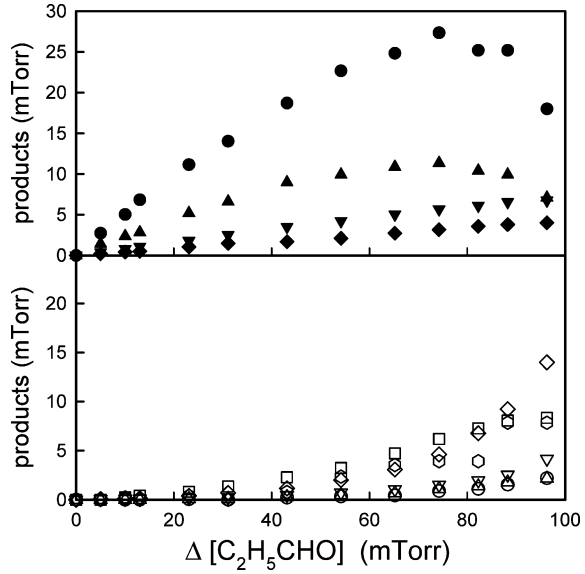

Figure 7. Panel A: formation of primary products CH_3CHO (circles), CH_3CH_2OOH (triangles), $CH_3CH_2C(O)OOH$ (inverted triangles), and $CH_3CH_2C(O)OH$ (diamonds) versus loss of CH_3CH_2CHO. Panel B shows formation of secondary products $CH_3C(O)OH$ (circles), $CH_3C(O)OOH$ (inverted triangles), HC(O)H (squares), HC(O)OH (diamonds), CH_3OH (triangles), and CH_3OOH (hexagons) obtained from successive UV irradiation of a mixture of 100 mTorr CH_3CH_2CHO and 216 mTorr Cl_2 in 700 Torr of air diluent.

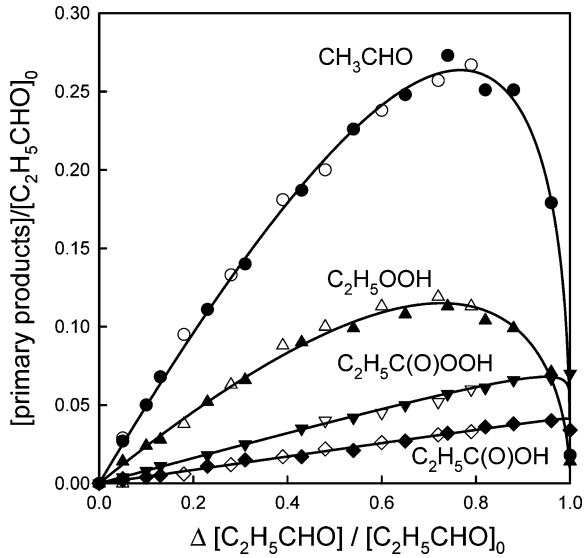

Figure 8. Formation of primary products CH_3CHO (circles), CH_3CH_2OOH (triangles), $CH_3CH_2C(O)OOH$ (inverted triangles), and $CH_3CH_2C(O)OH$ (diamonds) versus loss of CH_3CH_2CHO, normalized for the initial aldehyde concentration, following UV irradiation of mixtures of CH_3CH_2CHO and Cl_2 in 700 Torr of air. Open and filled symbols show results from different experiments. The lines through the data are fits of eq II to the data, see text for details.

The alkoxy radical then eliminates CO_2 to form the alkyl radical, CH_3CH_2, which will add O_2 and react with other peroxy radicals to give the ethoxy radical, CH_3CH_2O:

$$CH_3CH_2C(O)O + M \rightarrow CH_3CH_2 + CO_2 + M \quad (14)$$

$$CH_3CH_2 + O_2 + M \rightarrow CH_3CH_2O_2 + M \quad (15)$$

$$CH_3CH_2O_2 + RO_2 \rightarrow CH_3CH_2O + RO + O_2 \quad (38)$$

Finally, the ethoxy radical, CH_3CH_2O, reacts with oxygen to give the observed product, CH_3CHO.

$$CH_3CH_2O + O_2 \rightarrow CH_3CHO + HO_2 \quad (39)$$

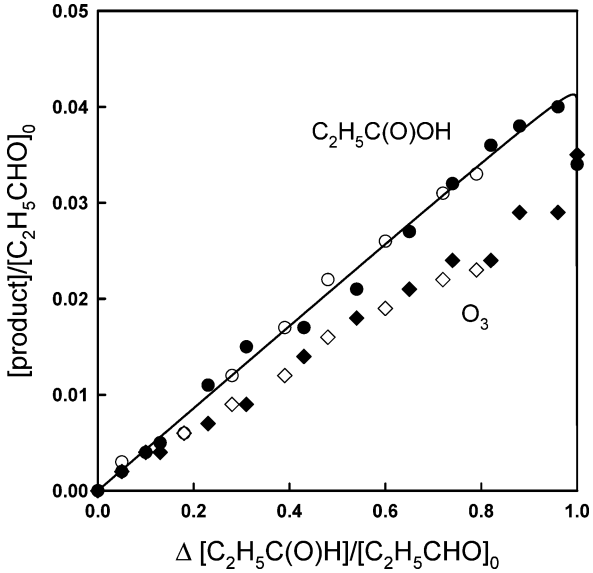

Figure 9. Formation of $CH_3CH_2C(O)OH$ (circles) and ozone (diamonds) versus the loss of CH_3CH_2CHO, normalized to the initial aldehyde concentration. Two experiments were performed in which mixtures of CH_3CH_2CHO and Cl_2 were irradiated in 700 Torr of air diluent.

3.6.2. $CH_3CH_2C(O)OH$ and $CH_3CH_2C(O)OOH$ as Primary Products. $CH_3CH_2C(O)OH$ and $CH_3CH_2C(O)OOH$ are observed as primary products of Cl initiated oxidation of CH_3CH_2CHO. The formation of these products is consistent with reactions 1a and 5 to form the propionylperoxy radical, $CH_3CH_2C(O)O_2$. By analogy to the established oxidation mechanism of CH_3CHO,[32] the reaction of propionylperoxy radicals with HO_2 proceeds via two channels forming the acid and the peracid:

$$CH_3CH_2C(O)O_2 + HO_2 \rightarrow CH_3CH_2C(O)OH + O_3 \quad (40a)$$

$$CH_3CH_2C(O)O_2 + HO_2 \rightarrow CH_3CH_2C(O)OOH + O_2 \quad (40b)$$

If reaction 40a is the source of $CH_3CH_2C(O)OH$, then ozone should be observed as a coproduct and should have a product profile similar to that of $CH_3CH_2C(O)OH$. Characteristic IR features of O_3 at 1000−1100 cm^{-1} were detected in the product spectra. Figure 9 shows a plot of the observed formation of ozone and $CH_3CH_2C(O)OH$ versus loss of the propionaldehyde, normalized for the initial aldehyde concentration. The initial yield of ozone is indistinguishable from that of $CH_3CH_2C(O)OH$ suggesting that reaction 40a is the source of both $CH_3CH_2C(O)OH$ and O_3. A more detailed interpretation of the ozone and $CH_3CH_2C(O)OH$ profiles in Figure 9 is complicated by three factors. First, the rate constant for the reaction of Cl atoms with O_3 is $k(Cl + O_3) = 1.2 \times 10^{-11}$ cm^3 $molecule^{-1}$ s^{-1}. By analogy to acetic acid, $k(Cl + CH_3C(O)OH) = 2.51 \times 10^{-14}$ cm^3 $molecule^{-1}$ s^{-1},[33] it is expected that the reactivity of Cl atoms toward ozone and $CH_3CH_2C(O)OH$ differs substantially, thereby complicating the analysis of the data in Figure 9. Second, for experiments employing significant consumptions of CH_3CH_2CHO, reaction of the primary product, CH_3CHO, with Cl will give $CH_3C(O)OH$ and O_3[32] thereby complicating the interpretation of the ozone yield. Finally, $CH_3CH_2C(O)OH$ is also produced in reaction 16b thereby complicating the interpretation of the propionic acid yield.

3.6.3. CH_3CH_2OOH as a Primary Product. The observation of the primary product, CH_3CH_2OOH, is consistent with formation of ethylperoxy radicals, $CH_3CH_2O_2$, with can then react with HO_2 to give the hydroperoxide, CH_3CH_2OOH.[34]

$$CH_3CH_2O_2 + HO_2 \rightarrow CH_3CH_2OOH + O_2 \quad (41)$$

Loss of the hydroperoxide via reaction with Cl atoms will produce CH_3CHO and probably explains why the value of k_{30} inferred from the measured ratio k_{30}/k_1 in section 3.6 above is approximately 30% lower than the accepted literature value.

3.6.4. Secondary and Tertiary Products. As shown in Figure 7b, acetic acid ($CH_3C(O)OH$), peracetic acid ($CH_3C(O)OOH$), methyl hydroperoxide (CH_3OOH), methanol (CH_3OH), formaldehyde (HC(O)H), and formic acid (HC(O)OH) were observed in yields which increased with the degree of CH_3CH_2CHO consumption. These are secondary and/or tertiary products of the Cl initiated oxidation of the propionaldehyde.

3.7. Infrared Spectrum of $CH_3CH_2C(O)O_2NO_2$ (PPN). The IR spectrum of $CH_3CH_2C(O)O_2NO_2$ was recorded by irradiating a mixture of 29.7 mTorr CH_3CH_2CHO, 103 mTorr Cl_2, and 11.6 mTorr NO_2 in 700 Torr of air. The reaction of Cl atoms with CH_3CH_2CHO in the presence of O_2 leads to the formation of propionylperoxy radicals. By analogy to the behavior of other acylperoxy radicals, it is expected that propionylperoxy radicals will react rapidly with NO_2 to give peroxypropionylnitrate, $CH_3CH_2C(O)O_2NO_2$.

$$CH_3CH_2CHO + Cl \rightarrow CH_3CH_2C(O) + HCl \quad (1a)$$

$$CH_3CH_2C(O) + O_2 + M \rightarrow CH_3CH_2C(O)O_2 + M \quad (5)$$

$$CH_3CH_2C(O)O_2 + NO_2 + M \rightarrow CH_3CH_2C(O)O_2NO_2 + M \quad (42,-42)$$

Peroxyacylnitrates are thermally unstable and decompose to reform acylperoxy radicals and NO_2. In the presence of excess NO_2 thermal decomposition of $CH_3CH_2C(O)O_2NO_2$ is masked by its reformation via reaction 42. Following UV irradiation of $CH_3CH_2CHO/Cl_2/NO_2$/air mixtures, a product was observed with IR features at 795, 852, 924, 965, 992, 1044, 1101, 1152, 1302, 1739, and 1834 cm^{-1} whose spectrum is shown in Figure 10a. The features shown in Figure 10a increased linearly with loss of CH_3CH_2CHO. The product features at 795, 1302, 1739, and 1834 cm^{-1} are characteristic of the NO scissors, NO_2 symmetric stretch, NO_2 asymmetric stretch, and CO stretching modes in peroxyacylnitrates, and we ascribe the spectrum in Figure 10a to $CH_3CH_2C(O)O_2NO_2$. For comparison, the spectrum of $CH_3C(O)O_2NO_2$ is shown in Figure 10b.

The addition of NO to the chamber once $CH_3CH_2C(O)O_2NO_2$ is formed results in the slow, dark decay of the peroxy nitrate due to a competition between the following reactions:

$$CH_3CH_2C(O)O_2 + NO_2 + M \rightarrow CH_3CH_2C(O)O_2NO_2 + M \quad (42,-42)$$

$$CH_3CH_2C(O)O_2 + NO \rightarrow \text{products} \quad (43)$$

The products formed during the decay of $CH_3CH_2C(O)O_2NO_2$ were acetaldehyde, ethyl nitrite, and ethyl nitrate through the following reactions:

$$CH_3CH_2C(O)O_2 + NO \rightarrow CH_3CH_2C(O)O + NO_2 \quad (44)$$

$$CH_3CH_2C(O)O + M \rightarrow CH_3CH_2 + CO_2 + M \quad (14)$$

$$CH_3CH_2 + O_2 + M \rightarrow CH_3CH_2O_2 + M \quad (15)$$

$$CH_3CH_2O_2 + NO \rightarrow CH_3CH_2O + NO_2 \quad (45)$$

$$CH_3CH_2O + NO \rightarrow CH_3CH_2ONO \quad (46)$$

$$CH_3CH_2O + NO_2 \rightarrow CH_3CH_2ONO_2 \quad (47)$$

$$CH_3CH_2O + O_2 \rightarrow CH_3CHO + HO_2 \quad (39)$$

Calibration of $CH_3CH_2C(O)O_2NO_2$ was achieved by equating the loss of the peroxy nitrate to the sum of the decay products observed. Using this calibration, the yield of peroxypropionylnitrate from the irradiation of the $CH_3CH_2CHO/Cl_2/NO_2$ mixture in 700 Torr air can be determined. Figure 11 shows the observed formation of $CH_3CH_2C(O)O_2NO_2$ versus the loss of CH_3CH_2CHO following successive UV irradiations. A linear least-squares fit to the data give a molar $CH_3CH_2C(O)O_2NO_2$ yield of (89 ± 5)%. This yield is consistent with the branching

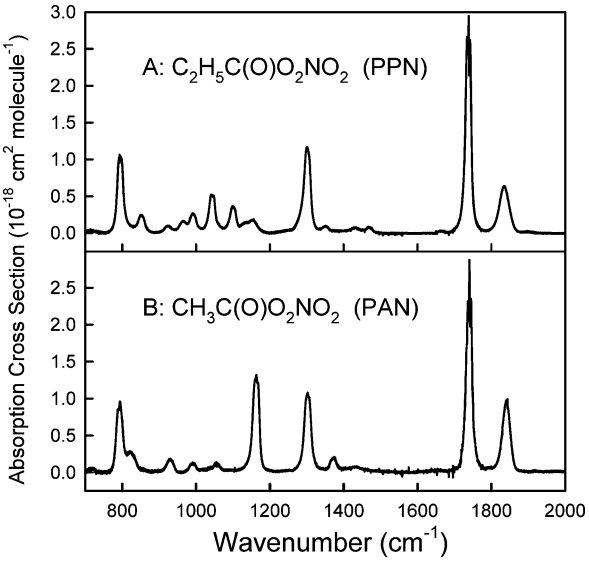

Figure 10. IR spectra of $CH_3CH_2C(O)O_2NO_2$ (A) and $CH_3C(O)O_2NO_2$ (B). $CH_3CH_2C(O)O_2NO_2$ has bands at 795, 1302, 1739, and 1834 cm^{-1}.

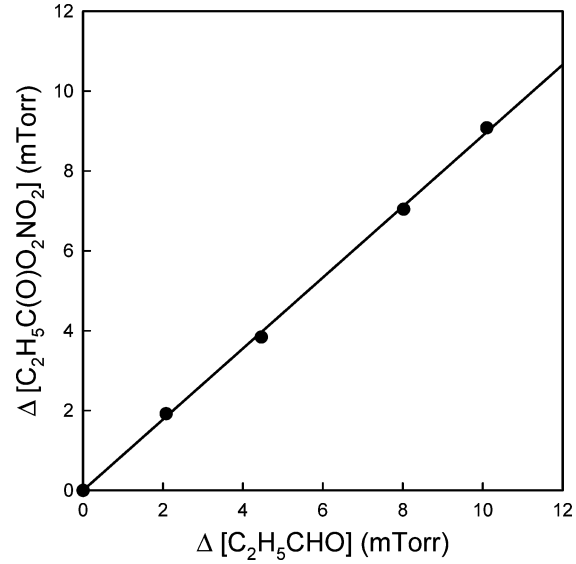

Figure 11. Formation of $CH_3CH_2C(O)O_2NO_2$ versus loss of CH_3CH_2CHO following successive UV irradiations of a $CH_3CH_2CHO/Cl_2/NO_2$ mixture in 700 Torr air. A linear least-squares fit gives a molar $CH_3CH_2C(O)O_2NO_2$ yield of (89 ± 5)%.

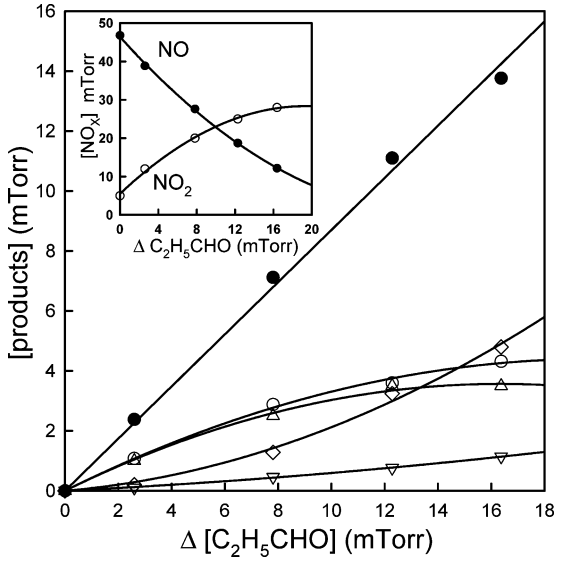

Figure 12. Formation of CH_3CHO (open circles), CH_3CH_2ONO (triangles), $CH_3CH_2ONO_2$ (inverted triangles), and $CH_3CH_2C(O)O_2NO_2$ (diamonds) versus loss of CH_3CH_2CHO following successive UV irradiations of a $CH_3CH_2CHO/Cl_2/NO/NO_2$ mixture in 700 Torr air. The NO (filled symbols) and NO_2 (open symbols) concentrations are shown in the insert. The sum of the four observed products is indicated by the filled circles and gives a composite yield of (87 ± 6)%.

ratio $\alpha_1 = k_{1a}/k_1 = 0.88$ reported in sections 3.4.1 and 3.4.2 with all peroxypropionylperoxy radicals reacting with NO_2 to give PPN.

3.8. Product Study of the Cl-Initiated Oxidation of CH_3CH_2CHO in the Presence of NO_x. Experiments were performed to investigate the mechanism of Cl atom initiated oxidation of CH_3CH_2CHO in the presence of NO_x. A mixture containing 37.2 mTorr CH_3CH_2CHO, 101 mTorr Cl_2, 47 mTorr NO, and 5 mTorr NO_2 in 700 Torr of air was introduced into the reaction chamber and irradiated using the UV blacklamps. Figure 12 shows the observed formation of CH_3CHO, CH_3CH_2ONO, $CH_3CH_2ONO_2$, and $CH_3CH_2C(O)O_2NO_2$ versus the loss of CH_3CH_2CHO following successive UV irradiations. The curvature of the product profiles reflects the changing NO and NO_2 concentrations, which are shown in the Figure 12 insert. The sum of the four observed products gives a composite yield of (87 ± 6)%, consistent with the four products resulting from abstraction of the aldehydic hydrogen.

The simplest explanation for the observed product distribution is the following sequence of reactions:

$$Cl + CH_3CH_2CHO \rightarrow CH_3CH_2C(O) + HCl \quad (1a)$$

$$CH_3CH_2C(O) + O_2 + M \rightarrow CH_3CH_2C(O)O_2 + M \quad (5)$$

$$CH_3CH_2C(O)O_2 + NO \rightarrow CH_3CH_2C(O)O + NO_2 \quad (44)$$

$$CH_3CH_2C(O)O + M \rightarrow CH_3CH_2 + CO_2 + M \quad (14)$$

$$CH_3CH_2 + O_2 + M \rightarrow CH_3CH_2O_2 + M \quad (15)$$

$$CH_3CH_2O_2 + NO \rightarrow CH_3CH_2O + NO_2 \quad (45)$$

$$CH_3CH_2O + O_2 \rightarrow CH_3CHO + HO_2 \quad (39)$$

Ethyl nitrite and ethyl nitrate are formed from the reaction of the ethoxy radical with NO and NO_2.

$$CH_3CH_2O + NO \rightarrow CH_3CH_2ONO \quad (46)$$

$$CH_3CH_2O + NO_2 \rightarrow CH_3CH_2ONO_2 \quad (47)$$

4. Discussion

4.1. Accuracy of Results from Flash Photolysis Experiments. Several factors influence the accuracy of the results obtained in the flash photolysis experiments. The chemistry associated with peroxy radical reactions is very complicated (see Tables 2 and 4). To quantify the sensitivity of the UV spectrum, of the self-reaction rate constant of the $CH_3CH_2C(O)O_2$ radical (Table 2), and of the branching ratio α_1 (Tables 2 and 4) to the parameters used for analysis, a systematic analysis of the propagation of errors was performed as described previously.[11]

The main sources of systematic errors on the UV spectrum of the $CH_3CH_2C(O)O_2$ radical arise from the calibration of the total initial radical concentration, from the absorption cross sections of HBr, and from the extrapolation of the fit to time zero. Calibration of the total radical concentration was achieved by replacing propionaldehyde by acetaldehyde keeping all other conditions constant. In the presence of CH_3CHO, Br atoms are converted into $CH_3C(O)O_2$ radicals whose absorption spectrum is well established.[18] Uncertainties associated with $\sigma(CH_3C(O)O_2)$ are estimated to be 20%, resulting in approximately 19% uncertainty in the absorption cross section of the $CH_3CH_2C(O)O_2$ radical at 207 nm. Uncertainties associated with σ(HBr) are estimated to be 30%, resulting in approximately 7.5% uncertainty in the absorption cross section of the $CH_3CH_2C(O)O_2$ radical. Uncertainties associated with the extrapolation of the fit to time zero is essentially due to the self-reaction rate constant of the $CH_3CH_2C(O)O_2$ radical (k_{13}) (fast initial decay). Uncertainties associated with k_{13} are estimated to be 34% resulting in approximately 9% of errors. Combining the uncertainties described above we estimate a global systematic uncertainty of 23% in the absorption cross section of the $CH_3CH_2C(O)O_2$ radical at 207 nm. A similar study has been conducted at 240 nm, and we estimate a global systematic uncertainty of 25% in the absorption cross section of the $CH_3CH_2C(O)O_2$ radical.

The main sources of systematic errors on the self-reaction rate constant of the $CH_3CH_2C(O)O_2$ radical arise from the absorption cross section value at 207 nm for the $CH_3CH_2C(O)O_2$ radical and from the rate constant of the ($CH_3CH_2C(O)O_2 + CH_3CH_2O_2$) cross-reaction. Variations of 23% in the $CH_3CH_2C(O)O_2$ absorption cross sections result in a variation of 32% in the value of k_{13}. Variation of 50% in the rate constant k_{16} results in a variation of 12% in k_{13}. Combining the uncertainties described above, we estimate a global systematic uncertainty of 34% in the k_{13} value.

Determination of the branching ratio α_1 depends on the calibration of the total initial radical concentration and on the absorption cross sections of $CH_3CH_2C(O)O_2$, $CH_2O_2CH_2CHO$, and CH_3CHO_2CHO radicals. Uncertainties associated with the $CH_3CH_2C(O)O_2$ cross sections are estimated to be 23%, resulting in approximately 20% uncertainty in the α_1 values. Uncertainties in the $CH_2O_2CH_2CHO$ and CH_3CHO_2CHO radical cross sections were estimated at 30% (spectra and uncertainties were assumed the same as for $CH_2O_2CH_2CH_3$ and $CH_3CHO_2CH_3$[35]). As discussed in our previous study on isobutyraldehyde

and pivalaldehyde,[10] the only examples of the influence of a carbonyl group on peroxy radical absorption reported in the literature are when the carbonyl is positioned α or β from the peroxy group (i.e., for $CH_3C(O)O_2$ and $CH_3C(O)CH_2O_2$), leading to the presence of two absorption bands.[36] In the case of $CH_2O_2CH_2CHO$ and CH_3CHO_2CHO, the carbonyl group is in the γ- and β-positions, i.e., remote from the peroxy chromophore, and it seems reasonable to assume that its influence will be small. As observed in the case of isobutyraldehyde,[10] no evidence for an additional absorption band around 210 nm was observed in the experimental curves corresponding to the propionaldehyde with Cl reaction in the presence of O_2, indicating that there is little (or no) effect of a γ-carbonyl group on the usual alkylperoxy band.

It should be noted that uncertainties in the mechanisms used to simulate experimental traces do not contribute to uncertainty in the branching ratio α_1. The ability of the simulations to fit the experimental data at 207 and 240 nm (see Figure 4) suggests that the reaction mechanism employed (see Tables 2 and 4) provides a reasonable description of the chemistry occurring in the system. Values of the propionylperoxy self-reaction rate constant obtained using Cl atom initiation were indistinguishable from those obtained using Br atom initiation. Rate constants for peroxy radical cross-reactions were obtained using either the geometric average of the self-reaction rate constants[25] in the case of alkylperoxy radicals or the value for the corresponding acetylperoxy radical reaction in the case of propionylperoxy radicals, as recommended by Villenave and Lesclaux.[26]

Finally, a variation of 34% in the $CH_3CH_2C(O)O_2$ self-reaction rate constant results in a variation of 8% in the value of α_1. Variations of the $CH_2O_2CH_2CHO$ and CH_3CHO_2CHO self-reaction rate constants by a factor of 2 result in a variation of only 1% in α_1. Allowing for an uncertainty of 50% in the rate constants for the cross-reactions ($CH_3CH_2C(O)O_2 + CH_2O_2CH_2CHO$ and $CH_3CH_2C(O)O_2 + CH_3CHO_2CHO$) results in an uncertainty of only 3% in the value of α_1. Variation of $k(CH_3CH_2C(O)O_2 + HO_2)$ over the range $1 \times 10^{-11}-2.5 \times 10^{-11}$ cm^3 molecule^{-1} s^{-1} did not change the value of the branching ratio. The insensitivity of α_1 to $k(CH_3CH_2C(O)O_2 + HO_2)$ reflects the small quantities of HO_2 present in the system. Combining the uncertainties described above we estimate a global systematic uncertainty of 22% in α_1.

4.2. Reactions of CH_3CH_2CHO with Cl Atoms and OH Radicals. *4.2.1. Reaction of CH_3CH_2CHO with Cl Atoms.* Rate constants for reactions of Cl atoms with propionaldehyde determined in the present work are in agreement, within the combined experimental uncertainties, with previous relative rate studies by Wallington et al.[37] $k_1 = (1.13 \pm 0.09) \times 10^{-10}$, Thévenet et al.[38] $k_1 = (1.4 \pm 0.3) \times 10^{-10}$, and Ullerstam et al.[39] $k_1 = (1.2 \pm 0.2) \times 10^{-10}$ cm^3 molecule^{-1} s^{-1}, all at room temperature.

The present study is the first investigation of the mechanism of the reaction of Cl atoms with propionaldehyde. We show that this reaction proceeds predominantly (88%) by abstraction of the aldehydic hydrogen atom. In a similar fashion, the reactions of Cl atoms with acetaldehyde, pivalaldehyde, and isobutyraldehyde proceed >95%,[8,9] (88 ± 6)%,[10] and (85± 5)%[10] via abstraction of the aldehydic hydrogen atom. Cl atoms are surprisingly selective in their reaction with aldehydes.

4.2.2. Reaction of CH_3CH_2CHO with OH Radicals. Seven previous measurements of the rate constant for the reaction of OH with propionaldehyde have been reported in the literature.[38,40−45] These values are compared with that measured in the present work in Table 5. There is an excellent agreement between the eight independent studies listed in Table 5, and it seems reasonable to conclude that the rate constant is known to within ±10%. There being no obvious reason to prefer any of the individual studies, we recommend the average of the individual determinations of $k(OH + CH_3CH_2CHO) = (1.91 \pm 0.19) \times 10^{-11}$ cm^3 molecule^{-1} s^{-1} for use in computer models of atmospheric chemistry.

TABLE 5: Comparison of $k(OH + CH_3CH_2CHO)$ Results

	year	technique	$k(OH + C_2H_5CHO)$ (10^{-11} cm^3 molecule^{-1} s^{-1})	k_{exp}/k_{av}
Niki et al.[40]	1978	RR[a]	2.1 ± 0.1	1.099
Kerr et al.[41]	1981	RR[a]	1.9 ± 0.4	0.995
Audley et al.[42]	1981	RR[a]	1.80 ± 0.21	0.942
Semmes et al.[43]	1985	RR[a]	1.71 ± 0.24	0.895
Papagni et al.[44]	2000	FP−RF[b]	2.02 ± 0.14	1.058
Thevenet et al.[38]	2000	PLP-LIF[b]	2.0 ± 0.3	1.047
D'Anna et al.[45]	2001	RR[a]	1.90 ± 0.15	0.995
this work	2004	RR[a]	1.82 ± 0.28	0.953
average			1.91	

[a] Relative rate measurement. [b] Flash photolysis − resonance fluorescence. [c] Pulsed laser photolysis − laser induced fluorescence.

4.3. UV Absorption Spectrum of the Propionylperoxy Radical. This is the first determination of the UV absorption spectrum of the propionylperoxy radical. This spectrum is similar to the UV absorption spectra of acetylperoxy,[18] isobutyrylperoxy,[16] and pivaloylperoxy[16] radicals, with the most intense absorption band at 207 nm ($\sigma_{207} = 6.71 \times 10^{-18}$ cm^2 molecule^{-1}) and one other band around 240 nm ($\sigma_{240} = 3.30 \times 10^{-18}$ cm^2 molecule^{-1}). The shape, the position, and the intensity of maxima of the UV absorption spectrum of the propionylperoxy radical are identical, within experimental uncertainties, to that of acetylperoxy,[18] isobutyrylperoxy,[16] and pivaloylperoxy[16] radicals, suggesting that the alkyl group R has a negligible effect on the UV spectra of the acylperoxy radicals $RC(O)O_2$. This observation provides a good indication that only the aldehydic H atoms are abstracted from reaction 2.

4.4. Self-Reaction of the Propionylperoxy Radical. The value of the self-reaction rate constant of the $CH_3CH_2C(O)O_2$ radical using Br atoms as an initiator ($k_{13} = (1.68 \pm 0.08) \times 10^{-11}$ cm^3 molecule^{-1} s^{-1}) measured in this work is in agreement with that measured by Bencsura et al.[46] ($k_{13} = (1.44 \pm 0.28) \times 10^{-11}$ cm^3 molecule^{-1} s^{-1}, using also Br as initiator) using a similar laser flash photolysis system coupled with UV absorption detection.

The $CH_3CH_2C(O)O_2$ self-reaction rate constant obtained using Cl atoms as an initiator ($k_{13} = (1.67 \pm 0.08) \times 10^{-11}$ cm^3 molecule^{-1} s^{-1}) is in excellent agreement with that measured using Br atoms. The kinetics of the $CH_3CH_2C(O)O_2$ self-reaction are similar to those measured for $CH_3C(O)O_2$, $(CH_3)_3CC(O)O_2$, $(CH_3)_2CHC(O)O_2$, and $C_6H_5C(O)O_2$ radicals.[10] In marked contrast to the behavior of RO_2 radicals,[35,47] the self-reaction kinetics of $RC(O)O_2$ radicals appears to be insensitive to the nature of the alkyl substituent R. This fact is convenient when modeling the atmospheric degradation of organic compounds which has not been the subject of detailed chemical study.

4.5. Infrared Spectrum of $CH_3CH_2C(O)O_2NO_2$. Table 6 compares the $CH_3CH_2C(O)O_2NO_2$ integrated band intensities obtained in this study with literature values. Gaffney et al.[48] do not state if the integrated band strengths are base e or base 10 values. However, when multiplied by 2.303, they compare well with the values of Picquet-Varrault et al.[49] and of the present work, suggesting that the reported values are base 10. The three IBI values for the 1301 cm^{-1} band agree to within 10% of their average. The integrated band strength (1700−1777 cm^{-1}) of

TABLE 6: Peroxypropionylnitrate Integrated Band Intensities (IBI, cm^2 molecule^{-1} cm^{-1})

band (cm^{-1})	integration limits (cm^{-1})	Gaffney et al.[48]	Picquet-Varrault et al.[49]	this work
796	760−830	1.97×10^{-17}		2.00×10^{-17}
1044	1010−1080	1.23×10^{-17}		1.17×10^{-17}
1301	1250−1340	2.86×10^{-17}	2.51×10^{-17}	2.88×10^{-17}
1738	1700−1777	5.03×10^{-17}		5.16×10^{-17}
1835	1777−1880	2.45×10^{-17}		2.62×10^{-17}

the NO_2 asymmetric stretching feature in $CH_3CH_2C(O)O_2NO_2$ determined herein is 5.16×10^{-17} cm^2 molecule^{-1} cm^{-1}, which is indistinguishable from that of $(5.14 \pm 0.10) \times 10^{-17}$ cm^2 molecule^{-1} cm^{-1} for the corresponding feature in $CH_3C(O)O_2NO_2$.[50] The integrated band strengths of the corresponding feature in $C_nF_{2n+1}C(O)O_2NO_2$ have been determined to be $(5.15 \pm 1.03) \times 10^{-17}$, $(5.25 \pm 1.04) \times 10^{-17}$, $(5.56 \pm 1.11) \times 10^{-17}$, and $(5.53 \pm 1.11) \times 10^{-17}$ cm^2 molecule^{-1} cm^{-1} for $n = 1$, 2, 3, and 4, respectively.[51,52]

5. Implications for Atmospheric Chemistry

Two independent and complementary experimental techniques were used to gather a large body of self-consistent data concerning the atmospheric chemistry of propionaldehyde. Reaction with Cl atoms proceeds rapidly with a rate constant which is within a factor of 4−5 of the gas kinetic limit. Abstraction of the aldehydic H-atom is the major (80−90%) reaction channel. When compared to the rest of the molecule, the aldehydic H-atom presents a relatively small target for incoming Cl atoms. As already observed for isobutyraldehyde and pivalaldehyde,[10] the selectivity and rapidity of aldehydic H-atom abstraction is remarkable given the unfavorable steric factors, suggesting that the reaction of Cl atoms with propionaldehyde probably does not proceed via a simple abstraction mechanism. In light of the electron density associated with the carbonyl group, the electrophilic nature of Cl atoms, and the proximity of the carbonyl group to the main reaction site (the aldehydic H-atom) it seems reasonable to speculate that the reaction may involve a short-lived complex in which the Cl atom is associated briefly with the carbonyl group before departing with the aldehydic H-atom. A computational study is needed to confirm or refute this suggestion.

As discussed in section 4.2.2, based upon the present work and the literature data, we recommend $k(OH + CH_3CH_2CHO) = (1.91 \pm 0.19) \times 10^{-11}$ cm^3 molecule^{-1} s^{-1}. The rate constant for reaction of Cl atoms with propionaldehyde is approximately 6 times greater than that with OH radicals. However, since the typical concentration of OH radicals in the troposphere exceeds that of Cl atoms by 2−3 orders of magnitude, loss of propionaldehyde via reaction with Cl atoms will be of negligible atmospheric importance. Using [OH] $= 1 \times 10^6$ cm^{-3} gives an atmospheric lifetime for propionaldehyde with respect to reaction with OH radicals of approximately 15 h. Photolysis is an important atmospheric loss mechanism for aldehydes. The lifetime of propionaldehyde depends on the solar zenith angle and is approximately 10−40 h for solar zenith angles of 0−60°.[23] Photolysis and reaction with OH are of comparable importance as atmospheric loss mechanisms for propionaldehyde. Uptake into water may also be an important fate for propionaldehyde in certain locations. However, on a global scale, contact of air with water (mainly in clouds) is a process which occurs on a time scale of 5−10 days and hence will not compete effectively with photolysis and reaction with OH. In most environments propionaldehyde will have an atmospheric lifetime < 1 day and will be removed by photolysis and reaction with OH radicals.

Photolysis of propionaldehyde in the lower atmosphere proceeds via C−C bond scission giving C_2H_5 and HCO radicals.[23] Reaction with OH is believed to proceed predominantly via abstraction of the aldehydic hydrogen to give propionyl radicals. In the present work we show that the atmospheric fate of propionyl radicals is addition of O_2 to give $CH_3CH_2C(O)O_2$ radicals. The kinetics of the self-reaction of $CH_3CH_2C(O)O_2$ radicals are indistinguishable from those of the acylperoxy radicals derived from other aldehydes studied to date (acetaldehyde, pivaldehyde ($(CH_3)_3CCHO$), and isobutyraldehyde).[53] In stark contrast to the behavior of RO_2 radicals, whose self-reaction rate constant decreases by 4 orders of magnitude on moving from R = CH_3 to R = $(CH_3)_3C$, the kinetics of the self-reaction of $RC(O)O_2$ radicals appear insensitive to the nature of the R group. At the present time, we recommend use of $k(CH_3C(O)O_2 + CH_3C(O)O_2) = k(RC(O)O_2 + RC(O)O_2) = k(RC(O)O_2 + R'C(O)O_2) = 2.9 \times 10^{-12} \exp(500/T)$ cm^3 molecule^{-1} s^{-1} [54,55] in computer models of global atmospheric chemistry.

Acknowledgment. The Bordeaux authors thank the French National Program for Atmospheric Chemistry for financial support.

References and Notes

(1) Andreini, B. P.; Baroni, R.; Galimberti, E.; Sesana, G. *Microchem. J.* **2000**, *67*, 11.
(2) Villanueva-Fierro, I.; Popp, C. J.; Martin, R. S. *Atmos. Environ.* **2004**, *38*, 249.
(3) Satsumabayashi, H.; Kurita, H.; Chang, Y. S.; Carmichael, G. R.; Ueda, H. *Atmos. Environ.* **1995**, *29*, 255.
(4) Viskari, E. L.; Vartiainen, M.; Pasanen, P. *Atmos. Environ.* **2000**, *34*, 917.
(5) Beine, H. J.; Jaffe, D. A.; Hering, J. A.; Kelley, J. A.; Krognes, T.; Stordal, F. *J. Atmos. Chem.* **1997**, *27*, 127.
(6) Chen, Y.; Zhu, L. *J. Phys. Chem. A* **2001**, *105*, 9689.
(7) Mallard, W. G.; Westley, F.; Herron, J. T.; Hampson, R. F.; Frizzel, D. H. NIST Chemical Kinetics Database, Version 6.0, NIST, Gaithersburg, MD, 1997.
(8) Bartels, M.; Hoyermann, K.; Lange, U. *Ber. Bunsen-Ges. Phys. Chem.* **1989**, *93*, 423.
(9) Niki, H.; Maker, P. D.; Savage, C. M.; Breitenbach, L. P. *J. Phys. Chem.* **1985**, *89*, 588.
(10) Le Crâne, J.-P.; Villenave, E.; Hurley, M. D.; Wallington, T. J.; Nishida, S.; Takahashi, K.; Matsumi, Y. *J. Phys. Chem. A* **2004**, *108*, 795.
(11) Lightfoot, P. D.; Lesclaux, R.; Veyret, B. *J. Phys. Chem.* **1990**, *94*, 700.
(12) Wallington, T. J.; Japar, S. M. *J. Atmos. Chem.* **1989**, *9*, 399.
(13) DeMore, W. B.; Sander, S. P.; Golden, D. M.; Hampson, R. F.; Kurylo, M. J.; Howard, C. J.; Ravishankara, A. R.; Kolb, C. E.; Molina, M. J. *NASA JPL Publ.* **1997**, 97−4.
(14) Hubinger, S.; Nee, J. B. *J. Photochem. Photobiol. A: Chem.* **1995**, *86*, 1.
(15) Kopitsky, R.; Willner, H.; Hermann, A.; Oberhammer, H. *Inorg. Chem.* **2001**, *40*, 2693.
(16) Tomas, A.; Villenave, E.; Lesclaux, R. *Phys. Chem. Chem. Phys.* **2000**, *2*, 1165.
(17) Jagiella, S.; Libuda, H. G.; Zabel, F. *Phys. Chem. Chem. Phys.* **2000**, *2*, 1175.
(18) Tyndall, G. S.; Cox, R. A.; Granier, C.; Lesclaux, R.; Moortgat, G. K.; Pilling, M. J.; Ravishankara, A. R.; Wallington, T. J. *J. Geophys. Res.* **2001**, *106*, 12157.
(19) Wine, P. H.; Semmes, D. H. *J. Phys. Chem.* **1983**, *87*, 3572.
(20) Wallington, T. J.; Hurley, M. D.; Ball, J. C.; Jenkin, M. E. *Chem. Phys. Lett.* **1993**, *211*, 41.
(21) Tyndall, G. S.; Orlando, J. J.; Wallington, T. J.; Dill, M.; Kaiser, E. W. *Int. J. Chem. Kinet.* **1997**, *29*, 43.
(22) Sander, S. P.; Friedl, R. R.; Golden, D. M.; Kurylo, M. J.; Huie, R. E.; Orkin, V. L.; Moortgat, G. K.; Ravishankara, A. R.; Kolb, C. E.; Molina, M. J.; Finlayson-Pitts, B. J. *JPL Publication No. 02-25*; NASA Jet Propulsion Lab.: Pasadena, CA, 2003.
(23) Calvert, J. G.; Atkinson, R.; Kerr, J. A.; Madronich, S.; Moortgat, G. K.; Wallington, T. J.; Yarwood, G. *The Mechanisms of Atmospheric Oxidation of the Alkenes*; Oxford University Press: 2000.
(24) Atkinson, R.; Baulch, D. L.; Cox, R. A.; Hampson, R. F., Jr.; Kerr, J. A.; Rossi, M. J.; Troe, J. Evaluated Kinetic and Photochemical Data for

Atmospheric Chemistry, Organic Species: Supplement VII. IUPAC Subcommittee on Gas Kinetic Data Evaluation for Atmospheric Chemistry. *J. Phys. Chem. Ref. Data* **1999**, *28*, 191.

(25) Villenave, E.; Lesclaux, R. *J. Phys. Chem.* **1996**, *100*, 14372.

(26) Villenave, E.; Lesclaux, R. *J. Geophys. Res.* **1998**, *103*, 25273.

(27) Meagher, R. J.; McIntosh, M. E.; Hurley, M. D.; Wallington, T. J. *Int. J. Chem. Kinet.* **1997**, *29*, 619.

(28) Crawford, M. A.; Wallington, T. J.; Szente, J. J.; Maricq, M. M. *J. Phys. Chem. A* **1999**, *103*, 365.

(29) Orlando, J. J.; Tyndall, G. S. *J. Photochem. Photobiol. A: Chem.* **2003**, *157*, 161.

(30) Hurley, M. D.; Sulbaek Andersen, M. P.; Wallington, T. J.; Ellis, D. A.; Martin, J. W.; Mabury, S. A. *J. Phys. Chem. A* **2004**, *108*, 615.

(31) Clague, A. D. H.; Bernstein, H. J. *Spectrochim. Acta* **1969**, *25A*, 593.

(32) Hasson, A. S.; Tyndall, G. S.; Orlando, J. J. *J. Phys. Chem. A* **2004**, *108*, 5979.

(33) Crawford, M. A.; Wallington, T. J.; Szente, J. J.; Maricq, M. M.; Francisco, J. S.; *J. Phys. Chem.* A **1999**, *103*, 365.

(34) Spittler, M.; Barnes, I.; Becker, K. H.; Wallington, T. J. *Chem. Phys. Lett.* **2000**, *321*, 57.

(35) Lightfoot, P. D.; Cox, R. A.; Crowley, J. N.; Destriau, M.; Hayman, G. D., Jenkin, M. E.; Moortgat, G. K.; Zabel, F. *Atmos. Environ., Part A* **1992**, *26*, 1805.

(36) Nielsen, O. J.; Johnson, M. S.; Wallington, T. J.; Christensen, L. K.; Platz, J. *Int. J. Chem. Kinet.* **2002**, *34*, 283.

(37) Wallington, T. J.; Skewes, L. M.; Siegl, W. O.; Wu, C.-H.; Japar, S. M. *Int. J. Chem. Kinet.* **1988**, *20*, 867.

(38) Thévenet, R.; Mellouki, A.; Le Bras, G. *Int. J. Chem. Kinet.* **2000**, *32*, 676.

(39) Ullerstam, M.; Ljungström, E.; Langer, S. *Phys. Chem. Chem. Phys.* **2001**, *3*, 986.

(40) Niki, H.; Maker, P. D.; Savage, C. M.; Breitenbach, L. P. *J. Phys. Chem.* **1978**, *82*, 132.

(41) Kerr, J. A.; Sheppard, D. W. *Environ. Sci. Technol.* **1981**, *15*, 960.

(42) Audley, G. J.; Baulch, D. L.; Campbell, I. M. J. *Chem. Faraday. Trans.* **1981**, *77*, 2541.

(43) Semmes, D. H.; Ravishankara, A. R.; Gump-Perkins, C. A.; Wine, P. H. *Int. J. Chem. Kinet.* **1985**, *17*, 303.

(44) Papagni, C.; Arey, J.; Atkinson, R. *Int. J. Chem. Kinet.* **2000**, *32*, 79.

(45) D'Anna, B.; Andresen, O.; Gefen, Z.; Nielsen, C. J. *Phys. Chem. Chem. Phys.* **2001**, *3*, 3057.

(46) Bencsura, Á.; Imrik, K.; Dóbé, S.; Bérces, T. *React. Kinet. Catal. Lett.* **2001**, *73*, 291.

(47) Wallington, T. J.; Dagaut, P.; Kurylo, M. J. *Chem. Rev.* **1992**, *92*, 667.

(48) Gaffney, J. S.; Fajer, R. Senum, G. I. *Atmos. Environ.* **1984**, *18*, 215.

(49) Picquet-Varrault, B.; Doussin, J.-F.; Durand-Jolibois, R.; Carlier, C. *Phys. Chem. Chem. Phys.* **2001**, 3, 2595.

(50) Tsalkani, N.; Toupance, G. *Atmos. Environ.* **1989**, *23*, 1849.

(51) Sulbaek Andersen, M. P.; Hurley, M. D.; Wallington, T. J.; Ball, J. C.; Martin, J. W.; Ellis, D. A.; Mabury, S. A.; Nielsen, O. J. *Chem. Phys. Lett.* **2003**, *379*, 28.

(52) Sulbaek Andersen, M. P.; Nielsen, O. J.; Hurley, M. D.; Ball, J. C.; Wallington, T. J.; Stevens, J. E.; Martin, J. W.; Ellis, D. A.; Mabury, S. A. *J. Phys. Chem. A* **2004**, *108*.

(53) Tomas, A.; Villenave, E.; Lesclaux, R. *J. Phys. Chem. A* **2001**, *105*, 3505.

(54) Atkinson, R. *Int. J. Chem. Kinet.* **1997**, *29*, 99.

(55) Atkinson, R.; Baulch, D. L.; Cox, R. A.; Crowley, J. N.; Hampson, R. F., Jr.; Hynes, R. G.; Jenkin, M. E.; Kerr, J. A.; Rossi, M. J.; Troe, J. Evaluated Kinetic and Photochemical Data for Atmospheric Chemistry, Organic Species: Supplement VII. IUPAC Subcommittee on Gas Kinetic Data Evaluation for Atmospheric Chemistry. Web version March 2005.